



NAVAL POSTGRADUATE SCHOOL

MONTEREY, CALIFORNIA

THESIS

**LONG-RANGE ATMOSPHERE-OCEAN FORECASTING IN
SUPPORT OF UNDERSEA WARFARE OPERATIONS IN
THE WESTERN NORTH PACIFIC**

by

Sarah L. Heidt

September 2009

Thesis Co-Advisors:

Tom Murphree
Rebecca E. Stone

Approved for public release, distribution is unlimited

REPORT DOCUMENTATION PAGE

Form Approved OMB No. 0704-0188

Public reporting burden for this collection of information is estimated to average 1 hour per response, including the time for reviewing instruction, searching existing data sources, gathering and maintaining the data needed, and completing and reviewing the collection of information. Send comments regarding this burden estimate or any other aspect of this collection of information, including suggestions for reducing this burden, to Washington Headquarters Services, Directorate for Information Operations and Reports, 1215 Jefferson Davis Highway, Suite 1204, Arlington, VA 22202-4302, and to the Office of Management and Budget, Paperwork Reduction Project (0704-0188) Washington DC 20503.

1. AGENCY USE ONLY (Leave blank)	2. REPORT DATE	3. REPORT TYPE AND DATES COVERED
	September 2009	Master's Thesis
4. TITLE AND SUBTITLE Long-range Atmosphere-Ocean Forecasting in Support of Undersea Warfare Operations in the Western North Pacific		5. FUNDING NUMBERS
6. AUTHOR(S) Sarah L. Heidt		8. PERFORMING ORGANIZATION REPORT NUMBER
7. PERFORMING ORGANIZATION NAME(S) AND ADDRESS(ES) Naval Postgraduate School Monterey, CA 93943-5000		
9. SPONSORING /MONITORING AGENCY NAME(S) AND ADDRESS(ES) N/A		10. SPONSORING/MONITORING AGENCY REPORT NUMBER
11. SUPPLEMENTARY NOTES The views expressed in this thesis are those of the author and do not reflect the official policy or position of the Department of Defense or the U.S. Government.		
12a. DISTRIBUTION / AVAILABILITY STATEMENT Approved for public release; distribution is unlimited		12b. DISTRIBUTION CODE

13. ABSTRACT (maximum 200 words)

Skillful long-range forecasts of acoustic variables have the potential to be very useful in planning Navy undersea warfare operations. Our study assessed the potential to predict sonic layer depth (SLD) in the western north Pacific at lead times of one to several months. We conducted correlations between SLD and remote climate system variables, and identified a high potential for skillful long-range forecasts of SLD in the western north Pacific using sea surface temperature in equatorial and south Pacific as predictors. We used tercile matching and composite analysis forecast (CAF) methods to develop hindcasts and forecasts of SLD based on SST predictors at lead times of one to four months. Our forecast verification metrics show that the resulting long lead probabilistic forecasts are a clear improvement over presently available long term mean climatology products. We also used conditional compositing techniques to create mean and environmental threshold probability products based on the long lead forecasts.

Our results indicate that the support of USW operations by the Navy meteorology and oceanography community could be improved by the use of advanced climate data sets, climate analysis, and long-range forecasting methods.

14. SUBJECT TERMS Sonic Layer Depth, Undersea Warfare, USW, Military Operations, Planning Timeframe, Anti-Submarine Warfare, ASW Western North Pacific, Climate, Climatology, Climate Analysis, Climate Prediction, Smart Climatology, Conditional Climatology, Long-range Forecast, Statistical Forecast, Simple Ocean Data Assimilation, SODA, Meteorology, Oceanography		15. NUMBER OF PAGES 99	
16. PRICE CODE			
17. SECURITY CLASSIFICATION OF REPORT Unclassified	18. SECURITY CLASSIFICATION OF THIS PAGE Unclassified	19. SECURITY CLASSIFICATION OF ABSTRACT Unclassified	20. LIMITATION OF ABSTRACT UU

NSN 7540-01-280-5500

Standard Form 298 (Rev. 8-98)
Prescribed by ANSI Std. Z39.18

THIS PAGE INTENTIONALLY LEFT BLANK

Approved for public release, distribution is unlimited

**LONG-RANGE ATMOSPHERE-OCEAN FORECASTING IN SUPPORT OF
UNDERSEA WARFARE OPERATIONS IN THE WESTERN NORTH PACIFIC**

Sarah L. Heidt
Lieutenant, United States Navy
B.S., United States Naval Academy, 2002

Submitted in partial fulfillment of the
requirements for the degrees of

MASTER OF SCIENCE IN PHYSICAL OCEANOGRAPHY
and
MASTER OF SCIENCE IN METEOROLOGY

from the

NAVAL POSTGRADUATE SCHOOL
September 2009

Author: Sarah L. Heidt

Approved by: Tom Murphree
Thesis Co-Advisor

Rebecca E. Stone
Thesis Co-Advisor

Jeffrey Paduan
Chairman, Department of Oceanography

Philip Durkee
Chairman, Department of Meteorology

THIS PAGE INTENTIONALLY LEFT BLANK

ABSTRACT

Skillful long-range forecasts of acoustic variables have the potential to be very useful in planning Navy undersea warfare operations. Our study assessed the potential to predict sonic layer depth (SLD) in the western north Pacific at lead times of one to several months. We conducted correlations between SLD and remote climate system variables, and identified a high potential for skillful long-range forecasts of SLD in the western north Pacific using sea surface temperature in equatorial and south Pacific as predictors. We used tercile matching and composite analysis forecast (CAF) methods to develop hindcasts and forecasts of SLD based on SST predictors at lead times of one to four months. Our forecast verification metrics show that the resulting long lead probabilistic forecasts are a clear improvement over presently available long term mean climatology products. We also used conditional compositing techniques to create mean and environmental threshold probability products based on the long lead forecasts.

Our results indicate that the support of USW operations by the Navy meteorology and oceanography community could be improved by the use of advanced climate data sets, climate analysis, and long-range forecasting methods.

THIS PAGE INTENTIONALLY LEFT BLANK

TABLE OF CONTENTS

I.	INTRODUCTION.....	1
	A. BACKGROUND	1
	B. EXISTING OPERATIONAL CLIMATE MONITORING AND FORECAST PRODUCTS FOR USW.....	2
	1. DoD Products.....	2
	a. <i>Navy Climatology</i>	2
	b. <i>Navy LRF and Planning Products for USW Operations</i>	2
	c. <i>Navy SRF Planning Products for USW Operations</i>	3
	d. <i>NAVO Experimental Climatology Products</i>	5
	2. Non-DoD Datasets and Methods	5
	3. Smart Climatology	7
	C. HOW CAN THE NAVY ATTAIN THE USW ADVANTAGE?	8
	1. Exploit the Battlespace on Demand Concept.....	8
	2. Re-evaluate Levels of Effort in USW Support	9
	3. Understand Planning Objectives and Timelines.....	10
	D. RESEARCH MOTIVATION AND SCOPE.....	11
	1. Prior Work	11
	2. Research Questions	13
	3. Thesis Organization	14
II.	DATA AND METHODS.....	15
	A. REGION AND PERIOD OF FOCUS	15
	1. Region	15
	2. Period	16
	B. SONIC LAYER DEPTH.....	17
	C. DATASETS AND SOURCES.....	19
	1. Simple Ocean Data Assimilation (SODA) Reanalysis.....	19
	2. NCEP/NCAR Atmospheric Reanalysis	21
	D. ANALYSIS AND FORECAST METHODOLOGY	22
	1. LTM and Standard Deviation of SLD	22
	2. Environmental Threshold Probabilities	23
	3. Predictands	23
	4. Correlations and Teleconnections	24
	5. Predictors	24
	6. Predictor and Predictand Time series	25
	7. Tercile Matching Forecast Method.....	25
	8. Composite Analysis Forecast.....	27
	9. Conditional Composite Climatologies	31
	E. SUMMARY OF CLIMATE ANALYSIS AND LONG-RANGE FORECAST METHODOLOGY	31
III.	RESULTS	33

A.	SEASONAL VARIATIONS IN THE WNP	33
1.	Winter	33
2.	Spring	35
3.	Summer	35
4.	Fall	37
B.	ENVIRONMENTAL FORECAST RESULTS BY REGION.....	37
1.	October East China Sea Region.....	37
2.	November ANNUALEX Region	51
C.	LONG-RANGE FORECASTS OF SONAR PERFORMANCE	64
IV.	CONCLUSION	65
A.	KEY RESULTS AND CONCLUSIONS	65
B.	APPLICABILITY TO DOD OPERATIONS.....	66
C.	AREAS FOR FURTHER RESEARCH	67
LIST OF REFERENCES.....		71
INITIAL DISTRIBUTION LIST		75

LIST OF FIGURES

Figure 1.	Sonic layer depth (ft): (a) analysis valid 00Z, 27 July 09, and (b) 72-hour forecast valid 00Z, 30 July 09. Black areas indicate a lack of valid data. Images from the Naval Oceanography Portal, July 2009.	4
Figure 2.	Depth excess (fathoms): (a) analysis valid 00Z, 27 July 09, and (b) 72-hour forecast valid 00Z, 30 July 09. Images from the Naval Oceanography Portal, July 2009.	4
Figure 3.	Sonic layer depth (ft) analysis from MOODS for: (a) March upper bound of the mean (95% confidence), and (b) March mean. Upper and lower bound of the mean are determined using the bootstrap method (e.g., Wilks 2006). Images from Krynen (2009).	5
Figure 4.	Battlespace on Demand (BonD) concept of operations for the Navy meteorology and oceanography community. Blue boxes describe smart climatology support products for each of the four BonD tiers. Adapted from Murphree (2008) and Evans (2008).	9
Figure 5.	Schematic representation of the present level of METOC effort in support of ASW planning and execution. Adapted from Murphree (2008) and based on a figure developed by J. Best and V. Gurley in 2005.	10
Figure 6.	Conditional composites of October mean surface vector wind (10 m level, in m/s) for the five years during 1970–2006 with the: (a) highest surface meridional wind speeds in the East China Sea, and (b) lowest surface meridional wind speeds in the East China Sea. From Turek (2008).....	12
Figure 7.	Conditional composites of October mean SLD (m) for the five years during 1970–2006 with the: (a) highest surface meridional wind speed in the East China Sea; and (b) lowest surface meridional wind speed in the East China Sea. Comparison of Figures 6 and 7 shows that higher (lower) meridional wind speeds tend to be associated with deeper (shallow) SLD. From Turek (2008).....	12
Figure 8.	Correlations between October 850 hPa meridional wind speed in the East China Sea and SST throughout the ocean at lead times of: (a) zero months, October wind with October SST; (b) one month, October wind with September SST; (c) two months, October wind with August SST; and (d) three months, October wind with July SST, based on reanalysis data from 1970–2006. Correlations with magnitudes greater than 0.314 are significant at the 95% level. Note the strong negative correlation in the Nino 4.0 index region (red box) at all lead times. Images created at ESRL web site, March 2009.	13

Figure 9.	Western north Pacific region of interest. This region is bounded by 0°–50°N and 100°–150°E. Image from Google maps [accessed online at http://maps.google.com/maps , July 2009].....	15
Figure 10.	Surface mean winds (m/s) for: (a) July, and (b) January in the WNP for 1970–2006. Images created at ESRL website, September 2009.	16
Figure 11.	Schematic of sound propagation in an ocean environment with a positive over negative vertical sound speed gradient. The depth of the near surface maximum sound speed is called the sonic layer depth (red line). Image adapted from (FAS), July 2009.....	18
Figure 12.	Schematic of sound propagation in an ocean environment with a negative vertical sound speed gradient and a sonic layer depth of zero. Image adapted from (FAS), July 2009.....	19
Figure 13.	Equations from the original NOAA CAF process used to calculate long-range forecasts of SLD in a predictand region using SST in a specified predictor region. Adapted from (MetEd), May 2009.....	29
Figure 14.	Equations used in modified CAF process to calculate long-range forecasts of SLD in a predictand region using analyzed AN SST predictor conditions.	30
Figure 15.	Flow chart showing main data sets and methods used to conduct climate analyses and long-range forecasting for this study.	32
Figure 16.	January (a) LTM of SLD (m), and (b) STD of SLD (m) in the WNP. The scales are different for this figure than for the corresponding figures for the other seasons (Figures 18, 19, and 20).	34
Figure 17.	(a) Schematic depiction of the Kuroshio and Oyashio depicted by black lines. The broken black line is the 1000 m contour and indicates the shelf break. As the Kuroshio encounters the Izu Ridge south of Honshu it negotiates along one of three paths depicted in red and green. (b) Time series indicating the annual variability in the Kuroshio paths. (c) Individual Kuroshio paths observed from summer 1976 to 1980. From Tomczak (2003).....	34
Figure 18.	April (a) LTM of SLD (m), and (b) STD of SLD (m) in the WNP. The scales are different for this figure than for the corresponding figures for January (Figure 16).	35
Figure 19.	July (a) LTM of SLD (m), and (b) STD of SLD (m) in the WNP. The scales are different for this figure than for the corresponding figures for January (Figure 16).	36
Figure 20.	October (a) LTM of SLD (m), and STD of SLD (m) in the WNP. The scales are different for this figure than for the corresponding figures for January (Figure 16).	37
Figure 21.	October SLD environmental threshold probabilities. Probability of SLD: (a) less than or equal to 5 meters; (b) greater than 5 meters and less than or equal to 25 meters; (c) greater than 25 meters and less than or equal to 46 meters; (d) greater than 46 meters and less than or equal to 70 meters; and (e) greater than 70 meters.	39

Figure 22.	October LTM SLD (m) showing three main October predictand regions used in this study. Large SLD potential predictand region indicated by red box (20° – 28° N, 122° – 126° E). Small SLD potential predictand region indicated by black box (25° – 26° N, 125° – 127.5° E). Multi-region SLD potential predictand region indicated by light blue and black boxes (22° – 24° N, 123° – 126° E, 24° – 25° N, 124° – 127° E, 25° – 26° N, 125° – 127.5° E, 26° – 27° N, 126° – 127.5° E). ...	40
Figure 23.	Correlations between the October ECS SLD predictand and SST in: (a) October; (b) September; (c) August; and (d) July, based on data from 1970–2006. Note the strong positive correlations in the central and eastern tropical Pacific. We chose the area of high positive correlations between 5° N– 5° S, 160° – 185° E (red box) as our potential predictor. For the October SLD predictand.	42
Figure 24.	Time series of ECS SLD predictand (blue line), October SST predictor (red line), and July SST predictor (green line) for 1970–2006.	43
Figure 25.	(a) Composite analysis for October SLD in the ECS using the equatorial-dateline SST predictor in July. Statistically significant results are outlined in black. (b) Corresponding probabilistic long-range hindcast of ECS SLD in October based on BN equatorial-dateline SST predictor in July. (c) Corresponding probabilistic long-range hindcast of ECS SLD in October based on AN equatorial-dateline SST predictor in July. For July 2009, the SST predictor values are AN (see Figure 26). Thus, our CAF prediction of October 2009 ECS SLD based on July 2009 equatorial-dateline SST conditions would be: probability of above normal SLD—58%; probability of near normal SLD—25%; and probability of below normal SLD—17%.....	45
Figure 26.	SST anomalies ($^{\circ}$ C) for July 2009. ECS equatorial-dateline SST predictor (red box). NAX south Pacific SST predictor (blue box). Image from (ESRL), July 2009.	46
Figure 27.	Conditional mean of October SLD based on compositing: (a) lower tercile July SST predictor years; (b) lower tercile October SLD predictand years; (c) upper tercile July SST predictor years; and (d) upper tercile October SLD predictand years.....	48
Figure 28.	October SLD threshold probabilities based on upper tercile July SST predictor years and upper tercile October SLD predictand years. Probability of SLD: (a) less than or equal to 5 meters using July SST predictor; (b) less than or equal to 5 meters using October SLD predictand; (c) greater than 5 meters and less than or equal to 25 meters using July SST predictor; and (d) greater than 5 meters and less than or equal to 25 meters using October SLD predictand. .	49
Figure 29.	October SLD threshold probabilities based on upper tercile July SST predictor years and upper tercile October SLD predictand years. Probability of SLD: (a) greater than 25 meters and less than	

or equal to 46 meters using July SST predictor; (b) greater than 25 meters and less than or equal to 46 meters using October SLD predictand; (c) greater than 46 meters and less than or equal to 70 meters using July SST predictor; (d) greater than 46 meters and less than or equal to 70 meters using October predictand; (e) greater than 70 meters using July SST predictor; and (f) greater than 70 meters using October SLD predictand.....	50
Figure 30. November (a) LTM of SLD (m), and (b) STD of SLD (m) in the WNP. The scales are different for this figure than for the corresponding figures for different months (Figures 16, 18–20).....	51
Figure 31. November SLD threshold probabilities showing probability of SLD: (a) less than or equal to 5 meters; (b) greater than 5 meters and less than or equal to 25 meters; (c) greater than 25 meters and less than or equal to 46 meters; (d) greater than 46 meters and less than or equal to 70 meters; (e) greater than 70 meters and less than or equal to 112 meters; and (f) greater than 112 meters. Based on ocean reanalysis data for 1970–2006.	52
Figure 32. November LTM SLD (m). ANNUALEX OPAREA indicated by black box (24° – 30.5° N, 128.5° – 134.5° E). Red (24° – 27° N, 128.5° – 131° E) and green (28.5° – 30.5° N, 132° – 134.5° E) boxes indicate potential SLD predictand regions within the larger ANNUALEX region.....	53
Figure 33. Correlations between November NAX SLD predictand and SST in: (a) November; (b) October; (c) September; (d) August; and (e) July based on data from 1970–2006. A positively correlated region (38° – 47° S, 210° – 230° E) in the Pacific was chosen as a potential predictor (black boxes).	55
Figure 34. Time series of November ANNUALEX SLD predictand (NAX, red line), November south Pacific SST predictor (light blue line), and July south Pacific SST predictor (dark blue line) for 1970–2006.	56
Figure 35. (a) Composite analysis for November SLD in ANNUALEX sub-region (NAX) using the south Pacific SST predictor in July. Statistically significant results are outlined in black or indicated by black arrows. (b) Corresponding probabilistic long-range hindcast of NAX SLD in November based on BN south Pacific SST predictor conditions in July. (c) Corresponding probabilistic long-range hindcasts of NAX SLD in November based on AN south Pacific SST predictor conditions in July. Thus, our CAF prediction of November 2009 NAX SLD based on AN July 2009 south Pacific SST conditions is: probability of above normal SLD—50%; probability of near normal SLD—50%; and probability of below normal SLD—0%.....	59
Figure 36. Conditional mean of November SLD based on compositing: (a) lower tercile July SST predictor years; (b) lower tercile November SLD predictand years; (C) upper tercile July SST predictor years; and (d) upper tercile November SLD predictand years.....	61

Figure 37. November SLD threshold probabilities based on upper tercile July SST predictor years and upper tercile November SLD predictand years. Probability of SLD: (a) less than or equal to 5 meters using July SST predictor; (b) less than or equal to 5 meters using November SLD predictand; (c) greater than 5 meters and less than or equal to 25 meters using July SST predictor; (d) greater than 5 meters and less than or equal to 25 meters using November SLD predictand; (e) greater than 25 meters and less than or equal to 46 meters using July SST predictor; (b) greater than 25 meters and less than or equal to 46 meters using November SLD predictand..... 62

Figure 38. November SLD threshold probabilities based on upper tercile July SST predictor years and upper tercile November SLD predictand years. Probability of SLD: (a) greater than 46 meters and less than or equal to 70 meters using July SST predictor; (b) greater than 46 meters and less than or equal to 70 meters using November predictand; (c) greater than 70 meters and less than or equal to 112 meters using July SST predictor; (d) greater than 70 meters and less than or equal to 112 meters using November SLD predictand; (e) greater than 112 meters using July SST predictor; and (f) greater than 112 meters using November SLD predictand..... 63

THIS PAGE INTENTIONALLY LEFT BLANK

LIST OF TABLES

Table 1.	Vertical levels (meters) analyzed by the Simple Ocean Data Assimilation (SODA) model.....	20
Table 2.	Schematic contingency table for hindcasts of AN SLD in October using SST in August as the predictor and assuming a positive correlation between the predictor and predictand. Note that hit, miss, FA, and CR values would be different for a different predictor and/or different predictand (e.g., BN SST predictor and AN SLD predictand).	26
Table 3.	Contingency table results and verification metrics from hindcasts generated using the tercile matching forecast method. Hindcasts of 1970–2006 October ECS SLD predictand based on equatorial-dateline SST predictor, with predictor leading by zero to three months. Columns A, B, C, and D represent the number of hits, false alarms, misses, and correct rejections respectively for AN, BN, and NN SLD values. See Chapter II, section D7, for details on contingency table and verification metrics.....	44
Table 4.	Contingency table results and verification metrics from hindcasts generated using the tercile matching method. Hindcasts of 1970–2006 NAX SLD predictand based on south Pacific SST predictor, with predictor leading by zero to four months. Columns A, B, C, and D represent the number of hits, false alarms, misses, and correct rejections respectively for AN, BN, and NN SLD values. See Chapter II, section D7, for details on contingency table and verification metrics.....	57

THIS PAGE INTENTIONALLY LEFT BLANK

LIST OF ACRONYMS AND ABBREVIATIONS

AN	Above normal
AOI	Area of interest
APC	Acoustic parameter climatology
ARGO	Advanced Research and Global Observation
ASW	Anti-submarine warfare
AVHRR	Advanced very high-resolution radiometer
BN	Below normal
BonD	Battlespace on Demand
BLG	Below layer gradient
CAF	Composite analysis forecast
CBLUG	Consolidated bottom loss upgrade
CNMOC	Commander, Naval Meteorology and Oceanography Command
COADS	Comprehensive Ocean-Atmosphere Data Set
COF	Cut-off frequency
CPC	Climate Prediction Center
CR	Correct rejection
CTF	Commander Task Force
DE	Depth excess
DoD	Department of Defense
ECMWF	European Center for Medium-range Weather Forecasts
ECS	East China Sea
ESRL	Earth Systems Research Laboratory
FA	False alarm
FARate	False alarm rate

GDEM	Generalized Digital Environmental Model
HFBL	High frequency bottom loss
hPa	Hecto-pascal
HSS	Heidke skill score
HVU	High value unit
ILG	In layer gradient
LRF	Long-range forecast
LTM	Long term mean
METOC	Meteorology and oceanography
MLD	Mixed layer depth
MODAS	Modular Ocean Data Assimilation System
MOODS	Master Oceanographic Observation Data Set
NASA	National Aeronautics and Space Administration
NAVO	Naval Oceanographic Office
NCAR	National Center for Atmospheric Research
NCEP	National Centers for Environmental Prediction
NCOM	Navy Coastal Ocean Model
NN	Near normal
NOAA	National Oceanic and Atmospheric Administration
NODC	National Oceanographic Data Center
NOGAPS	Navy Operational Global Atmospheric Prediction System
NPS	Naval Postgraduate School
ONI	Office of Naval Intelligence
OPAREA	Operational area
PC-IMAT	Personalized Curriculum for Interactive Multisensor Analysis Training
POD	Probability of detection

POP	Parallel Ocean Program
RIMPAC	Rim of the Pacific exercise
SLD	Sonic layer depth
SRF	Short range forecast
SODA	Simple Ocean Data Assimilation
SONAR	Sound navigation and ranging
SSH	Sea surface height
SSM/I	Special sensor microwave/imager
SST	Sea surface temperature
STD	Standard deviation
SV	Sound velocity
TAO/TRITON	Tropical Atmosphere-Ocean/Triangle Trans-Ocean Buoy Network
TDA	Tactical decision aid
USW	Undersea warfare
USWEX	Undersea warfare exercise
WHOI	Woods Hole Oceanographic Institute
WNP	Western North Pacific

THIS PAGE INTENTIONALLY LEFT BLANK

ACKNOWLEDGEMENTS

This thesis would not have been possible without the guidance and support of several individuals. I would like to first thank Dr. Tom Murphree for helping me to better understand our global climate system and instilling in me, an interest in the role climate research and technology has on the U.S. military. Your patience, guidance, scholarly advice, and thought provoking insight were instrumental in the completion of this research.

I would also like to thank CDR Rebecca Stone, USN, for her guidance and support; Mr. Bruce Ford from Clear Science Inc., for his generosity in providing the SODA dataset and for his programming advice; Mr. Mike Cook, for being able to understand what it was I wanted to program and helping me make that happen; and Mr. Bob Creasy, for all of his assistance in the Linux lab.

I also owe a large debt of gratitude to my parents, for always supporting and believing in me, and to my little brother for always making me laugh and for being the best brother a sister could ever have.

THIS PAGE INTENTIONALLY LEFT BLANK

I. INTRODUCTION

A. BACKGROUND

The mission of the Navy's meteorology and oceanography (METOC) community is to provide critical atmospheric and oceanographic information that will enhance commanders' awareness of the operational environment and the ability to exploit that awareness to gain an advantage across the range of military operations (Joint Staff 2008). This mission is particularly important when planning and executing undersea warfare (USW) operations and exercises, where small changes in the atmospheric and oceanic environment can have large impacts on acoustic sensor performance. Correctly forecasting the atmosphere and ocean at long lead times is imperative for the successful planning of operations in USW. Giving commanders a more realistic characterization of the battle space will allow for more informed decision making.

Understanding Earth's climate system is a critical factor in improving long-range forecasts (LRFs, forecasts with lead times of two weeks or longer). While the civilian community has taken many steps toward understanding climate variations and developing new forecasting technology, the Department of Defense (DoD) currently uses legacy climate products based on long term means (LTMs). Research by LaJoie (2006), Vorhees (2006), Hanson (2007), Moss (2007), Twigg (2007), Turek (2008), Crook (2009), and Ramsaur (2009), have all demonstrated the significance of using advanced climate data sets and methods to increase awareness at long lead times, of potential climate impacts on military operations. Several of these studies have led to the development of advanced forecasting techniques and resulted in viable LRFs of operationally significant regions (e.g., Iraq and Afghanistan).

This study will further explore how state of the science datasets, and advanced analysis and forecasting methods can be used to generate skillful LRFs for USW operations in the western north Pacific (WNP).

B. EXISTING OPERATIONAL CLIMATE MONITORING AND FORECAST PRODUCTS FOR USW

1. DoD Products

a. *Navy Climatology*

The Navy currently uses a LTM based, global ocean climatology database called Generalized Digital Environment Model (GDEM), in tactical decision aid (TDA) software, such as the Navy's Personalized Curriculum for Interactive Multisensor Analysis Training (PC-IMAT), to provide long lead tactical outlooks of the ocean environment for USW planning. GDEM climatology is derived using temperature and salinity profiles from the Modular Ocean Data Assimilation System (MODAS), which uses optimum interpolation and statistical regression to generate synthetic temperature and salinity profiles from remotely sensed sea surface temperature (SST) and height (SSH) and from in situ measurements extracted from the Master Oceanographic Observational Data Set (Carnes 2003; Fox et al., 2002). GDEM (V3.0) consists of monthly climatologies of temperature, standard deviation of temperature, salinity, and standard deviation of salinity, at $\frac{1}{4}$ -degree horizontal resolution with 78 vertical depths from the surface to 6600 meters (Carnes 2003). LTM based climatology datasets, like GDEM, are common, and very useful, but by the nature of their definition, many important temporal aspects of the climate system, such as trends and oscillations (e.g., El Nino and La Nina), are invariably smoothed out. Since LTM based climatologies cannot account for climate system variations, using them for long-range forecasting and operational planning in regions and periods where such variations occur can be problematic. Refer to Turek (2008) for further information on GDEM and PC-IMAT.

b. *Navy LRF and Planning Products for USW Operations*

In recent USW exercises, Navy planning briefs tend to lack extensive climate analysis in the form of environmental characterization at lead times of two weeks or more. The *USS John C Stennis USWEX 09* planning brief

provided sonic layer depth (SLD) and cut-off frequency (COF) LTM climatology plots using MOODS data for the month of operation (February). Additional probability of detection (POD) plots for various sensors at predetermined target depths and frequencies were generated using the Navy Coastal Ocean Model (NCOM) with valid times of 11 January 2009 @ 0000Z (John C Stennis 2009). These products provide standardized and familiar visualizations to the commander, but the combination of LTM climatology for February and snapshots of current model conditions (11 January) for an exercise occurring in one month is not optimal when we know the effects of monthly variability that can exist in the climate.

The critical features assessment brief for the FOAL EAGLE 09 exercise described SLD, COF, and depth excess (DE) in broad general statements with minimal reference as to where this information was derived. Additional figures displaying consolidated bottom loss upgrade (CBLUG) and high frequency bottom loss (HFBL) for the region of interest were presented; but, again, with minimal reference to the source or the forecast valid time (Foal Eagle 2009). These statements are not intended to claim that current long-range support is not helpful for USW planning purposes, but are intended to point out shortcomings in long lead DoD climate support that can be readily addressed.

c. Navy SRF Planning Products for USW Operations

While there is much to be done in the development of better long-range planning support for USW operations, extensive work has been done to develop advanced short range forecasts for use within 72 hours of the start of operations. For both exercises previously mentioned, USWEX 09 and FOAL EAGLE 09, explicit short range forecasts out to 72 hours, based on NCOM were issued. NCOM provides ocean nowcasts and forecasts at a range of lead times

and horizontal resolutions (72 hours and 1/8-degree) Figure 1 and Figure 2 show examples of short range NCOM products, produced by the Naval Oceanographic Office (NAVO), of derived acoustic variables for a specific USW exercise region.

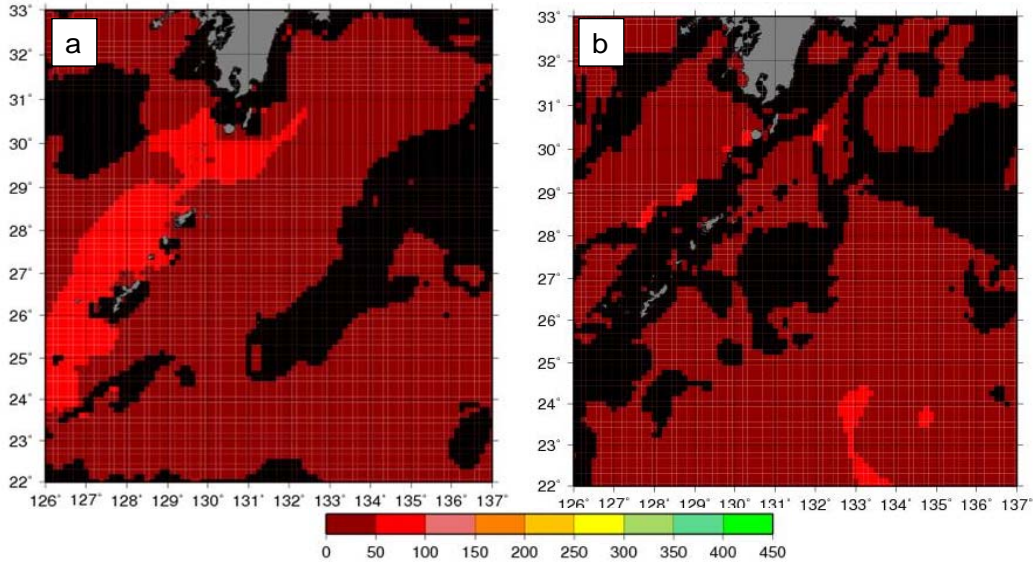


Figure 1. Sonic layer depth (ft): (a) analysis valid 00Z, 27 July 09, and (b) 72-hour forecast valid 00Z, 30 July 09. Black areas indicate a lack of valid data. Images from the Naval Oceanography Portal, July 2009.

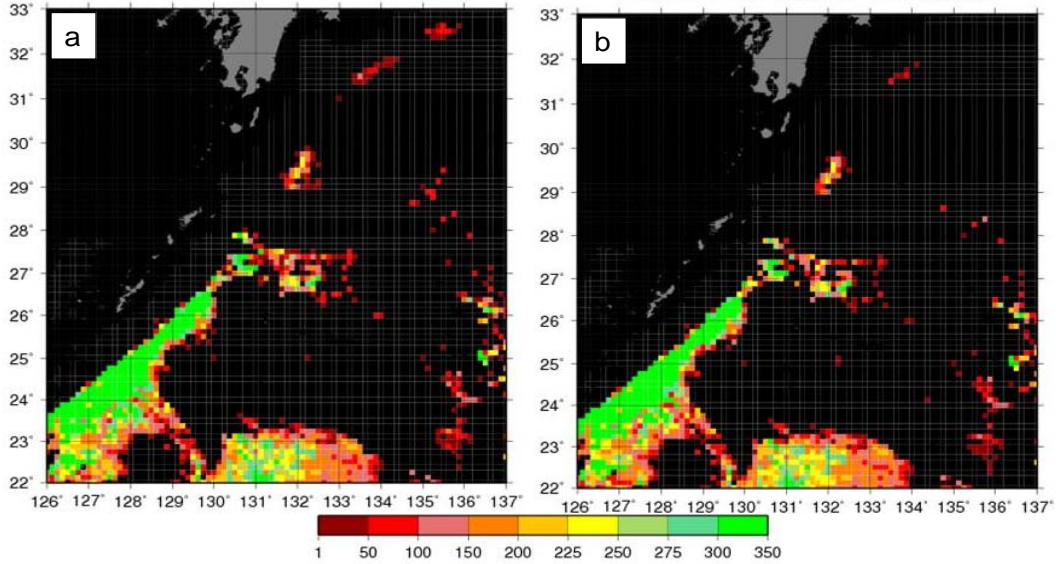


Figure 2. Depth excess (fathoms): (a) analysis valid 00Z, 27 July 09, and (b) 72-hour forecast valid 00Z, 30 July 09. Images from the Naval Oceanography Portal, July 2009.

d. NAVO Experimental Climatology Products

The Navy is aware of the shortcomings in their current long-range USW support products and NAVO has taken the initiative to expand and develop new products, using new technology and analysis methods. Figure 3 shows an example of experimental acoustic parameter climatology (APC) products created at NAVO. These products are derived from individual in situ MOODS profiles. For locations with a sufficient number of profiles, various long-term monthly mean statistical quantities are calculated at $\frac{1}{4}$ degree resolution for SLD, mixed layer depth (MLD), below layer gradient (BLG), deep sound channel axis, and critical depth (Krynen 2009).

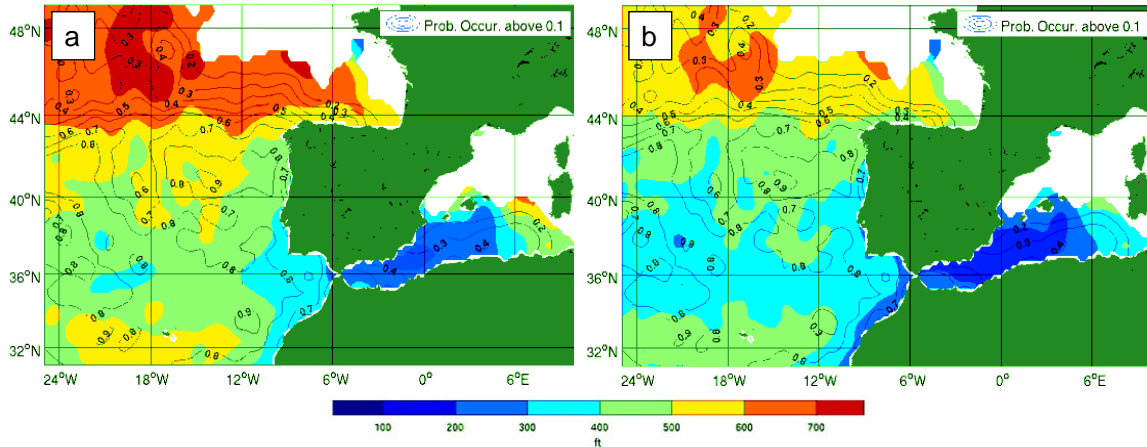


Figure 3. Sonic layer depth (ft) analysis from MOODS for: (a) March upper bound of the mean (95% confidence), and (b) March mean. Upper and lower bound of the mean are determined using the bootstrap method (e.g., Wilks 2006). Images from Krynen (2009).

APC database files are accessible to METOC support personnel, and APC products similar to those in Figure 3 have been included in long-range planning products for some USW exercise planning conferences and in new sensor development by the Office of Naval Intelligence (ONI) (Krynen 2009).

2. Non-DoD Datasets and Methods

Civilian agencies, such as the National Oceanic and Atmospheric Administration (NOAA) Climate Prediction Center (CPC), and Earth System

Research Laboratory (ESRL) have surpassed the Department of Defense in their use of state of the science technology to develop advanced datasets and methods to analyze and forecast the climate system. In many cases, this technology is freely available to the public. However, the Navy has adapted and used very little of this technology to advance Navy climate prediction capabilities. ESRL provides public access to a number of climate datasets through their interactive, web-based plotting and analysis tools. These tools, and an atmospheric reanalysis dataset developed by the National Centers for Environmental Prediction (NCEP) and the National Center for Atmospheric Research (NCAR), were extensively used in our study and will be further discussed in Chapter II.

In this study, it is important to differentiate between a state of the science reanalysis dataset and a LTM-based climatology dataset. In our study, we used the NCEP/NCAR atmospheric reanalysis dataset and the Simple Ocean Data Assimilation (SODA) ocean reanalysis dataset. Unlike LTM based climatology datasets (e.g., GDEM), reanalysis datasets are constructed by integrating observations obtained from numerous data sources together within a numerical prediction model, through a process called data assimilation (CCSP 2008). The result is a continuous and spatially uniform, reconstructed analysis of past atmospheric and/or oceanic conditions, typically spanning 30 years or longer.

Ocean reanalysis datasets, like SODA, have significant advantages over LTM based datasets, like GDEM, because of their explicit representation of atmospheric and ocean dynamics, and their much higher temporal resolution that can capture climate variations and other temporal fluctuations of the atmosphere and ocean. While GDEM uses statistical analysis methods to fill in data gaps in space and time, SODA resolves data gaps in a dynamically consistent and more realistic manner (Turek 2008). More information on SODA and the use of it in our study will be discussed in Chapter II.

3. Smart Climatology

The smart climatology concept, developed by Dr. Tom Murphree and Rear Admiral David Titley, uses state of the science basic and applied climatology to directly support DoD operations (Murphree 2008). Smart climatology uses state of the science climatology datasets (e.g., NCEP/NCAR and SODA reanalyses) and methods (e.g., conditional compositing, teleconnection analyses, statistical and dynamical prediction systems) to analyze, monitor, and forecast the climate system (Murphree 2008).

A number of smart climatology studies conducted at the Naval Postgraduate School have demonstrated that significant improvements could be made in METOC support for Navy operations by adapting advanced datasets and methods. These include studies by Turek (2008) and Ramsaur (2009) that identified smart climatology improvements in climate scale support for USW operations in the WNP. Several of these studies have developed and tested systems for producing operational long-range forecasts of the environment, and of radar and sonar performance, in areas of high priority for the DoD, such as Iraq (Hanson 2007; Crook 2009), Afghanistan (Moss 2007), Korea (Tournay 2007), the Indian Ocean (Twigg 2007), the North Atlantic (Raynak 2009), and the WNP (Mundhenk 2009; Ramsaur 2009). In all of these studies, smart climatology has proven to be a viable concept for improving METOC support at long lead times across a variety of military operations.

In this study, we have extended the research done by Turek (2008) in which he compared smart ocean climatologies with traditional Navy climatologies including comparisons of their impacts on long-range predictions of acoustic variables and sonar performance. Turek (2008) determined that there was a high potential for smart climatology to improve such long-range predictions, but he did not actually develop and test a long-range prediction system. In our study, we built upon the findings of Turek (2009) and used state of the science

datasets, analysis, and LRF methods, to develop and test techniques for operationally generating feasible and tactically significant LRF products in support of USW operations in the WNP.

C. HOW CAN THE NAVY ATTAIN THE USW ADVANTAGE?

Locating a submarine in the Pacific Ocean has often been described as trying to find a needle in a haystack. Stealthy tactics of an adversary, a noisy medium, and limited U.S. capabilities, put USW operators at a significant disadvantage when it comes to detecting subsurface targets. Thus, it is imperative that the Navy design, develop, test, and produce concepts and products that can give USW operators the best chance at successfully accomplishing their mission. This section outlines ideas for how this can be achieved.

1. Exploit the Battlespace on Demand Concept

The Battlespace on Demand (BonD) concept developed by the Commander, Naval Meteorology and Oceanography Command (CNMOC) presents a strategy for achieving decision superiority for the warfighter through the exploitation of information about the battlespace environment (Evans 2008). The BonD concept has four tiers, as depicted in Figure 4. Tier zero represents observations, consisting of environmental data from an array of sources (e.g., in situ and remote measurement systems). Tier one represents analyses and predictions of the environment based on data from tier zero. Tier two represents predictions of how environmental conditions described in tier one affect the performance of military equipment (e.g., sensors, communication, and weapons systems). Tier three represents recommendations on how to best exploit environmental opportunities and mitigate environmental risks.

The BonD concept was originally developed to help improve short range environmental support for warfighters. However, the concept applies equally well to long-range support. The blue text boxes in Figure 4 identify smart climatology products we associate with each of the four BonD tiers. In this study, we have

applied advanced climate datasets and methods at the tier zero level to develop LRFs for USW at the tier one level. These LRFs form the foundation for the subsequent development of long-range support at the tier two and three levels.

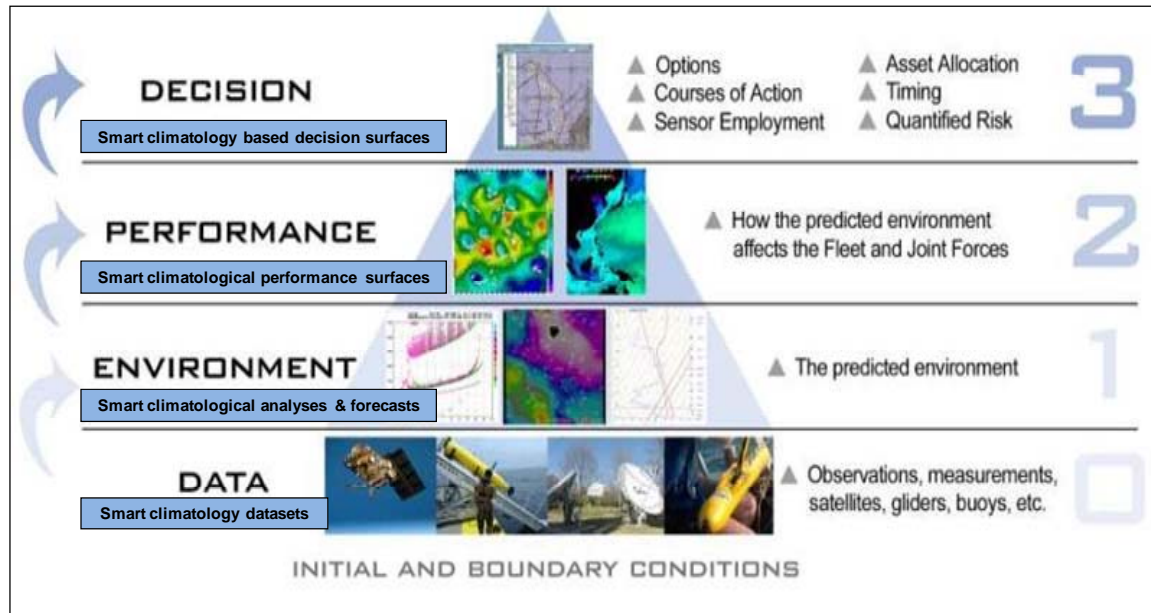


Figure 4. Battlespace on Demand (BonD) concept of operations for the Navy meteorology and oceanography community. Blue boxes describe smart climatology support products for each of the four BonD tiers. Adapted from Murphree (2008) and Evans (2008).

2. Re-evaluate Levels of Effort in USW Support

In an anti-submarine warfare (ASW) coordination and concept of operations brief given in March 2005, CAPT Best (then the CNMOC Director for ASW) and CDR Gurley (then the CNMOC Deputy Director for ASW) described the present levels of METOC effort in support of planning and execution of ASW operations, and the resulting levels of impact. This is depicted in Figure 5 in which the blue line represents the level of effort for METOC support at lead times of years to hours and the red line represents the level of impact this support has on overall operations. Notice that, in this ASW example, relatively little effort is spent on METOC support at lead times of one week to two months (i.e., intraseasonal climate support). This large dip in METOC support occurs when ASW commanders are making major operational decisions regarding resources,

platform assignments, deployment load-outs, and training (Murphree 2008). This is when large amounts of money are allocated for operations, and this is where the greatest opportunity exists for long-range METOC support products to significantly contribute to the success of ASW operations. The implication of the analysis by Best and Gurley shown in Figure 5 is that skillful LRFs of the environment and equipment performance could significantly improve METOC support, and the impacts of that support, at weekly to seasonal lead times when major ASW decisions are being made.

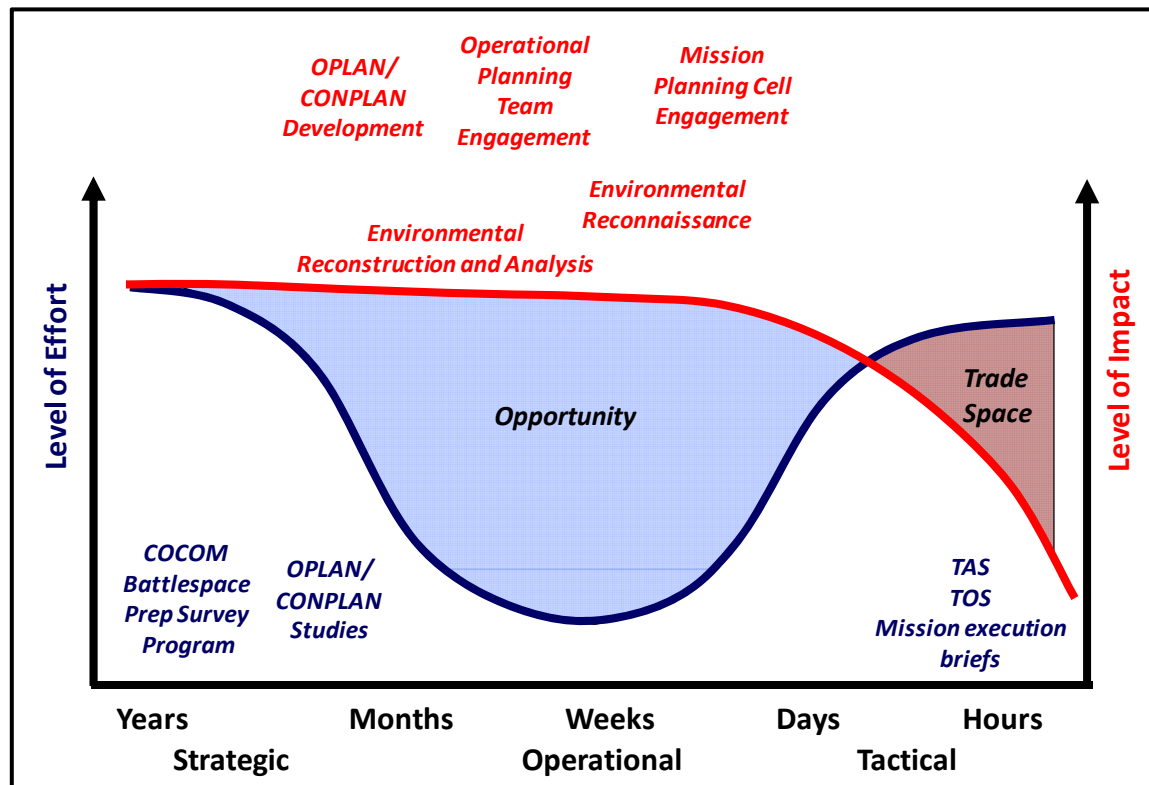


Figure 5. Schematic representation of the present level of METOC effort in support of ASW planning and execution. Adapted from Murphree (2008) and based on a figure developed by J. Best and V. Gurley in 2005.

3. Understand Planning Objectives and Timelines

In order to give timely and accurate long-range forecasts to USW planners, forecasters must first understand what types of decisions are made at long lead times, and how their LRF products can best support those decisions

and overall mission objectives. Typical mid-phase planning conference discussions for USW related operations occur three to six months prior to the start of operations and include: friendly asset assignments, target asset discussions, expected atmospheric and oceanic conditions, environmental characterization, sensor deployment, sensor performance, and active/pассиве SONAR ranges. Knowing this, Navy forecasters must strive to provide forecasts at lead times of three to six months that will enable decision makers to better understand the operational environment, including environmental uncertainties, and make decisions that will maximize sensor performance, give friendly forces the acoustic advantage, and give the high value unit (HVU) maximum defensibility. A major goal of our study was to develop and test techniques for generating such long-range forecasts.

D. RESEARCH MOTIVATION AND SCOPE

1. Prior Work

A major motivation for conducting our research on climate analyses and long-range forecasting for USW operations in the WNP was the research completed by Turek (2008) and preliminary research conducted in NPS climatology courses. Turek (2008) showed that smart climatology processes could be used to significantly improve the climatological characterization of the ocean environment for tactical exploitation. Figure 6 and Figure 7 show results from Turek (2008) that indicate a strong relationship between surface winds and SLD in the WNP, in particular in the East China Sea (ECS). Notice that higher (lower) surface meridional wind speeds tend to be associated with deeper (shallow) SLDs. Turek (2008) demonstrated that these wind-driven differences in SLD lead to tactically significant variations in sonar performance.

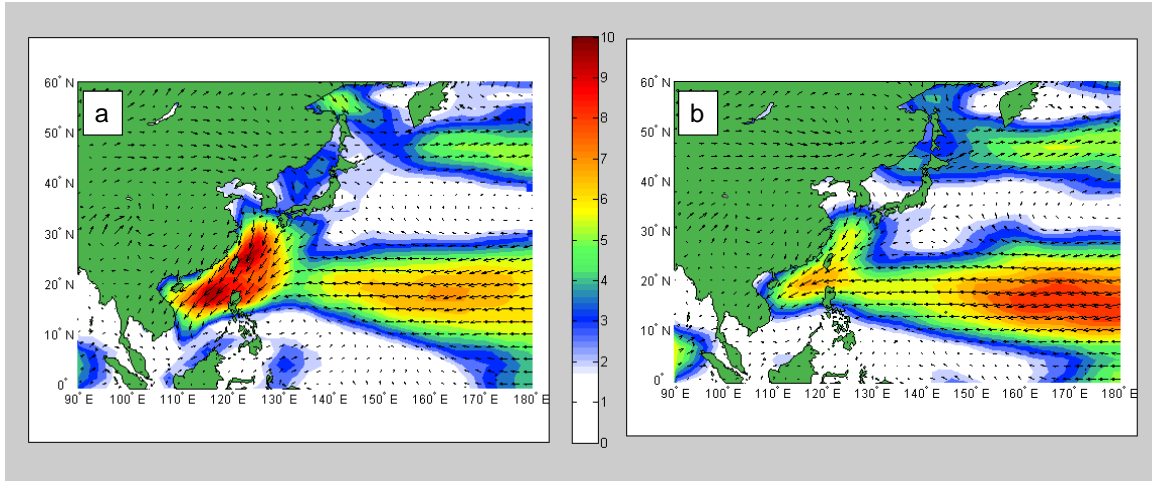


Figure 6. Conditional composites of October mean surface vector wind (10 m level, in m/s) for the five years during 1970–2006 with the: (a) highest surface meridional wind speeds in the East China Sea, and (b) lowest surface meridional wind speeds in the East China Sea. From Turek (2008).

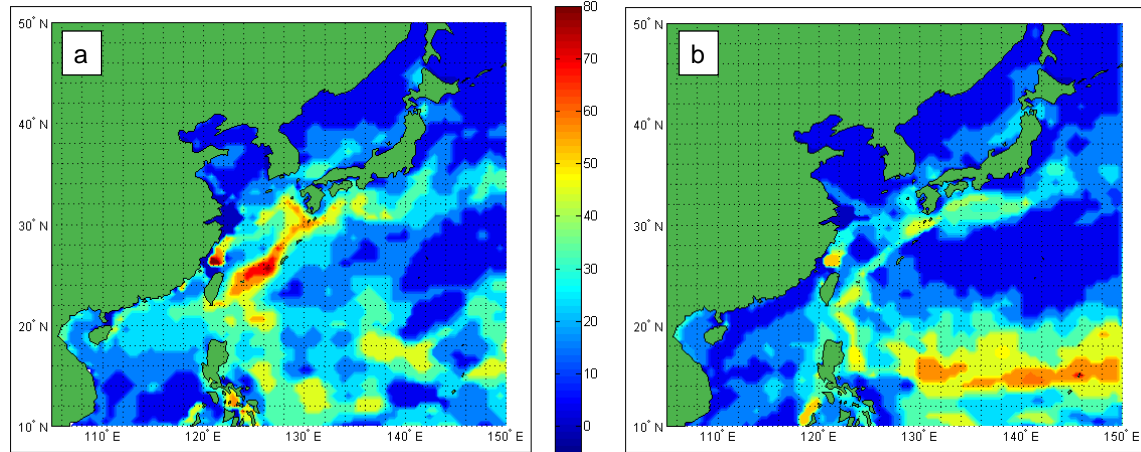


Figure 7. Conditional composites of October mean SLD (m) for the five years during 1970–2006 with the: (a) highest surface meridional wind speed in the East China Sea; and (b) lowest surface meridional wind speed in the East China Sea. Comparison of Figures 6 and 7 shows that higher (lower) meridional wind speeds tend to be associated with deeper (shallow) SLD. From Turek (2008).

Though Turek (2008) did not investigate long lead forecasting, our preliminary research showed significant correlations between SST in the equatorial Pacific and winds in the ECS region (Figure 8) at lead times of several

months, and suggested there was a high potential for skillful long-range forecasting of SLD using SST as a predictor. In this study, we explored that potential.

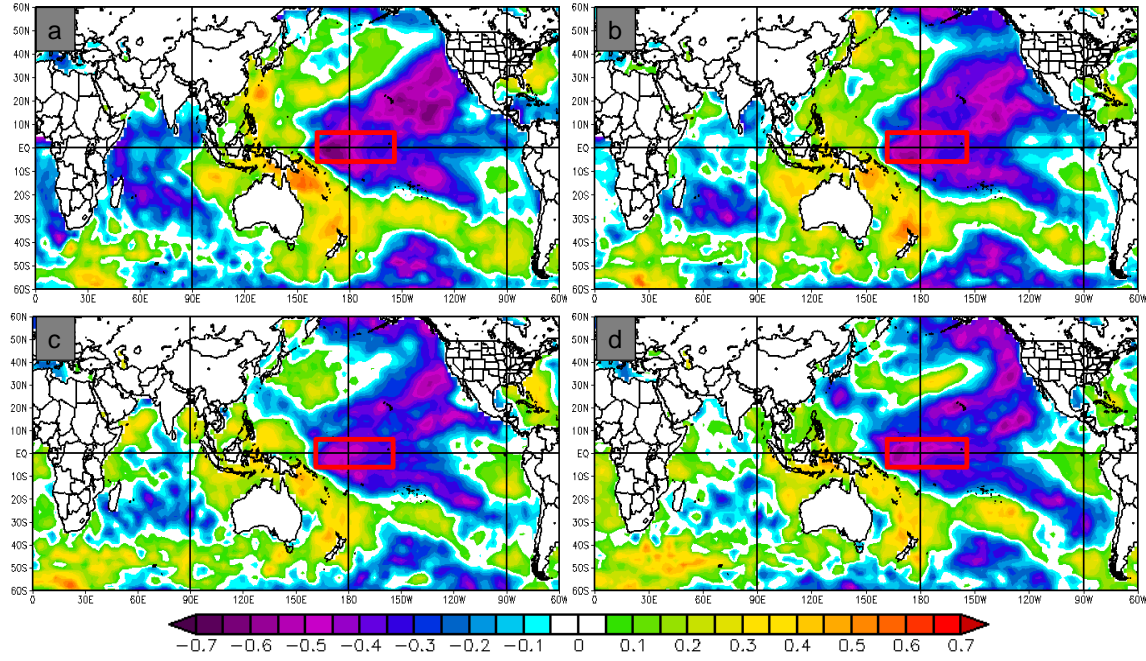


Figure 8. Correlations between October 850 hPa meridional wind speed in the East China Sea and SST throughout the ocean at lead times of: (a) zero months, October wind with October SST; (b) one month, October wind with September SST; (c) two months, October wind with August SST; and (d) three months, October wind with July SST, based on reanalysis data from 1970–2006. Correlations with magnitudes greater than 0.314 are significant at the 95% level. Note the strong negative correlation in the Nino 4.0 index region (red box) at all lead times. Images created at ESRL web site, March 2009.

2. Research Questions

This study explored the viability of using smart climatology datasets and methods to skillfully forecast atmospheric and oceanic conditions at long lead times, in order to provide warfighters with significantly enhanced capabilities for exploiting the environment as they plan and conduct USW operations. This study focuses primarily on investigating the following questions:

- 1) What atmospheric and oceanic variables in the WNP are both operationally significant and predictable at long lead times?
- 2) What atmospheric and oceanic variables are the most viable predictors of climate variations in the WNP, and can these variables be used to skillfully predict oceanic conditions at long lead times?
- 3) What are the skill and operational value of LRFs in planning, supporting, and conducting USW operations in the WNP?

3. Thesis Organization

In order to answer these research questions, we focused on a systematic approach to conducting climate analysis, and to developing long-range forecasting products for USW operations in the WNP.

Chapter II begins by defining the study region and period of interest, and then provides an overview of the two reanalysis datasets used in this study, as well as the methods and analysis tools used to develop and test LRFs in support of USW operations in the WNP. Chapter III provides an overview of seasonal variations in SLD and outlines results for two specific forecast regions, chosen based on scientific and operational factors. Chapter IV provides a summary of our results and conclusions, and offers suggestions for future research.

II. DATA AND METHODS

A. REGION AND PERIOD OF FOCUS

1. Region

We chose the western north Pacific (WNP) region shown in Figure 9 as our focus region in this study.



Figure 9. Western north Pacific region of interest. This region is bounded by 0° – 50° N and 100° – 150° E. Image from Google maps [accessed online at <http://maps.google.com/maps>, July 2009].

There were two specific reasons for choosing this region. First, the WNP is a region of large-scale climate variations in both the atmosphere and the ocean. This is largely due to the southwest and northeast monsoon wind regimes, illustrated in Figure 10, which dominate the summer and winter months respectively. Second, the WNP and its marginal seas are of great

tactical and strategic interest to the United States. We conducted analyses and developed LRFs for the WNP as a whole and for specific regions within the WNP based on scientific and operational factors.

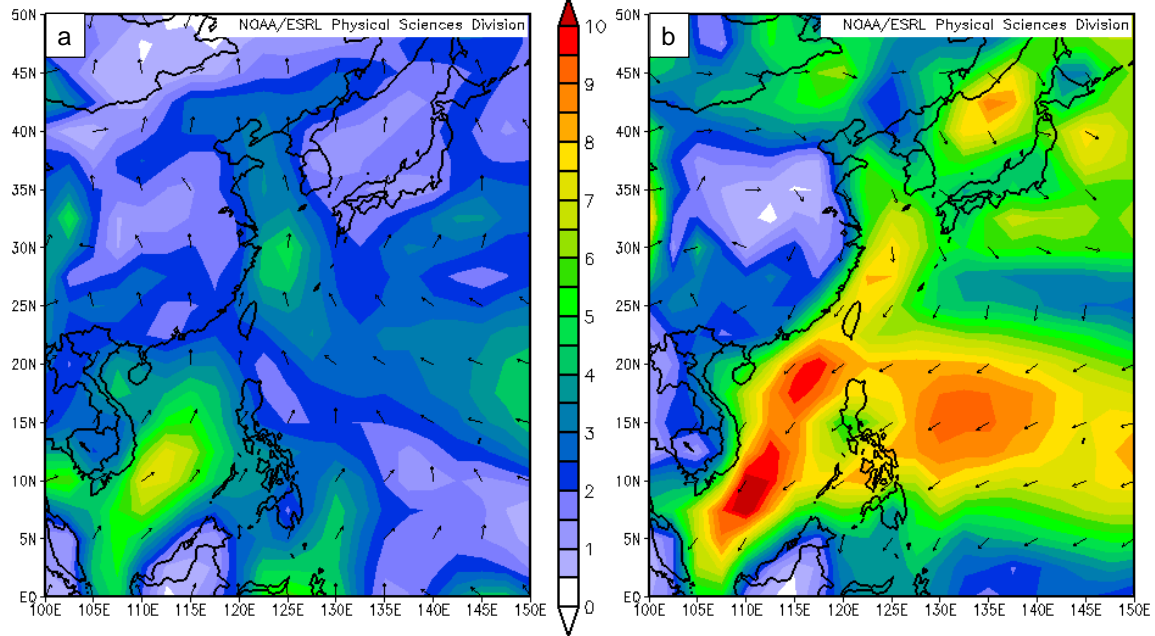


Figure 10. Surface mean winds (m/s) for: (a) July, and (b) January in the WNP for 1970–2006. Images created at ESRL website, September 2009.

2. Period

This study encompasses a 37 year period from 1970–2006. This period was chosen based on the availability of data from both the NCEP and SODA reanalysis datasets. While data does exist prior to 1970, we chose to maximize the positive impacts of satellite data and exclude pre-satellite era years for data consistency within this study. From research by Vorhees (2006) and Ford (2000), we also know that this time-period captures a number of intraseasonal to interannual climate variations (e.g., Madden-Julian Oscillation, El Nino, La Nina) as well as some representation of decadal variations. We conducted seasonal climate analyses for the WNP region based on the months of January (winter),

April (spring), July (summer), and October (fall). We also conducted analyses and developed LRFs for specific months (e.g., October, November) based on scientific and operational factors.

B. SONIC LAYER DEPTH

Undersea warfare depends heavily on knowledge of the ocean acoustic environment. Environmental characterization for USW planning is typically based on acoustic variables, such as sound velocity (SV), sonic layer depth (SLD), below layer gradient (BLG), in layer gradient (ILG), and cut off frequency (COF). For this study, we chose to focus on sonic layer depth as our predictand or forecast variable. SLD is defined as the near surface level of maximum sound velocity, and is highly dependent on ocean temperature. To have a non-zero sonic layer depth generally requires a neutral or positive temperature gradient. Turek (2008) showed that sonic layer depth is closely correlated to surface wind speed, with deep (shallow) SLDs associated with strong (weak) surface winds. This association is due to wind forcing of ocean heat fluxes, mixing, and circulations and the resulting impacts on ocean temperature.

A deep SLD denotes the existence of a surface duct that may be of sufficient depth to trap or duct a certain range of acoustic frequencies. This can be beneficial for producing longer detection ranges, particularly for active sonar frequencies. The down side, however, is that the very qualities that allow the surface duct to trap sound above the SLD also make it difficult for sound to penetrate the SLD from below. This means that a signal originating from below the SLD may be undetectable by sensors deployed above the SLD (Turek 2008). Figure 11 shows a sound velocity profile with a positive vertical sound speed gradient overlying a negative vertical sound speed gradient; the red line indicates the sonic layer depth. Sound above this layer refracts toward the surface creating a surface duct and sound that makes it below this layer refracts downward toward minimum sound velocity, producing a shadow zone, depicted by the gray region.

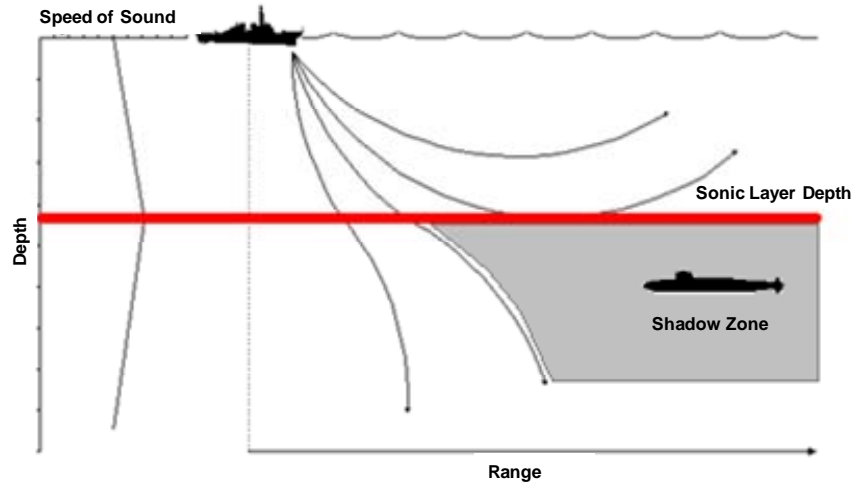


Figure 11. Schematic of sound propagation in an ocean environment with a positive over negative vertical sound speed gradient. The depth of the near surface maximum sound speed is called the sonic layer depth (red line). Image adapted from (FAS), July 2009.

There are instances in which the maximum near surface sound velocity is at the surface and the formation of a surface duct is not possible. In this situation, a negative vertical sound velocity gradient exists with a SLD at zero depth, and all sound refracts downward towards regions of minimum sound velocity. This type of acoustic environment is typically associated with decreasing temperature with depth, which often occurs in summer months when winds are calm and turbulent mixing is minimal (Turek 2008). Initially, one might think this would be ideal for detecting subsurface targets, but as sound propagates downward and bends toward minimum sound velocity, a near surface shadow zone is created (see Figure 12).

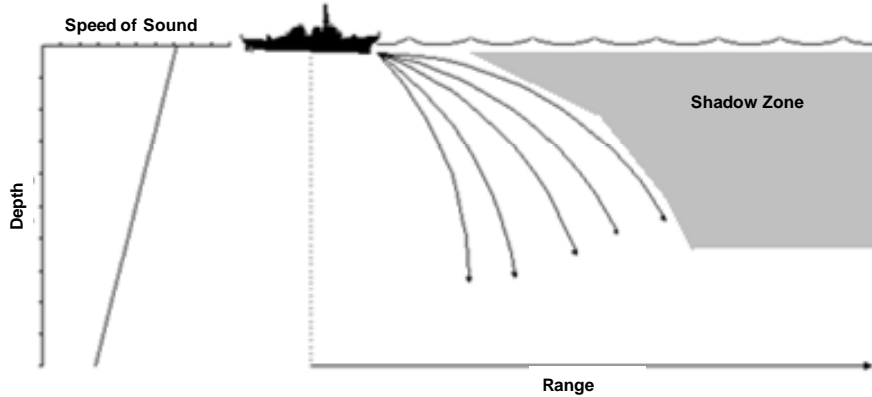


Figure 12. Schematic of sound propagation in an ocean environment with a negative vertical sound speed gradient and a sonic layer depth of zero. Image adapted from (FAS), July 2009.

C. DATASETS AND SOURCES

1. Simple Ocean Data Assimilation (SODA) Reanalysis

SODA is a global retrospective analysis of ocean variables that extends from January 1958 to within a few years of the present (Carton et al., 2000). SODA was created to reconstruct historical ocean climate variability on space and timescales similar to those captured by the NCEP/NCAR atmospheric reanalysis project. For this study, we used SODA reanalysis output variables from version 2.0.2 for years 1970–2001, and version 2.0.4 for years 2002–2006. Both versions have an identical temporal resolution of five days, a global domain covering 72.25°S–89.25°N and 0°–360°E, and 40 vertical levels between 5 and 5374 meters in depth (Table 1). The SODA output variables for these two versions are temperature (°C), salinity (psu), sea surface height (m), zonal and meridional ocean velocity (m/s), and wind stress (N/m²). These variables are available in various forms from the Asia Pacific Data Research Center (APDRC 2009a,b).

Table 1. Vertical levels (meters) analyzed by the Simple Ocean Data Assimilation (SODA) model.

SODA DEPTHS (meters)			
5	129	729	3124
15	148	918	3374
25	171	1139	3624
35	197	1378	3874
46	229	1625	4124
57	268	1875	4374
70	317	2125	4624
82	381	2375	4874
96	465	2624	5124
112	579	2874	5374

The SODA ocean reanalysis uses a numerical model, driven by observation based surface forcing, to provide a first guess of the evolving ocean state. At assimilation time, a set of error estimation equations are used to correct the first guess. The general circulation model used by the SODA system is based on Parallel Ocean Program (POP) numerics, with displaced poles, to allow for resolution of arctic processes. The model uses 1/30° bathymetry analysis; K-profile parameterization for diffusion of momentum, heat, and salt; daily surface winds provided by the ECMWF-40 reanalysis; and surface freshwater fluxes provided by the Global Precipitation Climatology Project (Carton and Giese 2008).

The in situ observational data used to develop the SODA reanalysis include almost all available hydrographic profile data, as well as ocean station data, moored temperature and salinity time series, and surface temperature and salinity observations of various types. Two-thirds of this data was obtained from the World Ocean Database 2001 but also included are observations from the National Oceanographic Data Center (NODC)/NOAA temperature archive; the

Tropical Atmosphere-Ocean/Triangle Trans-Ocean buoy Network (TAO/TRITON) mooring thermistor array; ARGO (Advanced Research and Global Observation) drifter data from Woods Hole Oceanographic Institute (WHOI); and bucket temperatures from the Comprehensive Ocean-Atmosphere Data Set (COADS). To account for nonrandom errors, a series of quality control filters are applied to temperature and salinity profiles; observations exceeding the analysis by up to three standard deviations are rejected (Carton and Giese 2008).

The satellite data used to develop the SODA reanalysis includes NOAA/National Aeronautics and Space Administration (NASA) Advanced Very High Resolution Radiometer (AVHRR) operational SST measurements. Only nighttime retrieval data is used in order to reduce error associated with skin temperature affects. Satellite altimetry data are used in SODA versions 1.4.3 and higher, and QuickSCAT wind data are used in SODA version 2.0.4 (Carton and Giese 2008).

For this study, we used SODA monthly mean output values of temperature and salinity for the years 1970–2006 to derive corresponding acoustically relevant variables of interest for USW operations. Sound velocity was calculated using the nine-term McKenzie (1981) sound velocity equation from SODA depth, temperature, and salinity variables. Sonic layer depth was calculated using a MATLAB function created by Turek (2008). Once SLD was calculated uniformly across all years of interest, we calculated LTM, standard deviation, and environmental threshold probabilities using MATLAB. Our ability to resolve vertical variations in temperature, salinity, sound speed, and other quantities was constrained by the levels at which SODA variables were available (Table 1). Thus, our SLD values were limited to occurring at one of the SODA depths, rather than at intermediate depths.

2. NCEP/NCAR Atmospheric Reanalysis

The NCEP/NCAR atmospheric reanalysis dataset is the product of a 40-year global, retrospective analysis of atmospheric fields from January 1948 to

present. The reanalysis uses a spectral statistical interpolation (SSI) analysis module and a T62/28-level global spectral model for data assimilation (Kalnay et al., 1996). Observations collected for this reanalysis consist of global rawinsonde data, Comprehensive Ocean-Atmosphere Data Set (COADS) surface marine data, aircraft data, surface land synoptic data, satellite sounder data, Special Sensor Microwave/Imager (SSM/I) surface wind speeds, and satellite cloud drift winds. All data is subject to advanced quality control checks and run through an advanced monitoring system (Kalnay et al., 1996).

NCEP/NCAR reanalysis output is available at a temporal resolution of six hours on a uniform horizontal grid with a spatial resolution of 2.5° at all standard tropospheric and stratospheric levels, including sea surface temperature (Kistler et al., 2001). We chose to use this dataset for our study based on its ability to capture low frequency climate variations; its accessibility; and for the availability of NCEP/NCAR's advanced plotting and data analysis tools. In our study we used data from 1970–2006 to be consistent with data used from the SODA ocean reanalysis dataset. Throughout this study, the NCEP/NCAR reanalysis plotting and analysis tools were used to develop predictor and predictand indices, and to identify correlations on which to base long-range climate forecasts to support USW planning. Further discussion of how this was accomplished and what variables were used from this reanalysis dataset are presented in the methodology portion of this chapter.

D. ANALYSIS AND FORECAST METHODOLOGY

1. LTM and Standard Deviation of SLD

Using monthly SODA ocean reanalysis data, the 37-year long term mean and standard deviation (STD) of sonic layer depth were calculated for the WNP region. This was done to identify seasonal cycles and to interpret and identify processes that might be associated with, or the cause of, seasonal variations in sonic layer depths in the WNP region. These calculations also helped us identify

regions of high and low variability, and gave us a better understanding of the LTM climatology of operationally significant regions for USW planning.

2. Environmental Threshold Probabilities

Environmental thresholds are often used in the military to determine whether and how to conduct an operation. For example, a threshold of 12 foot wave heights might be used to determine whether a surface ship can safely and effectively conduct an operation. In our study, we chose to take a similar approach to calculate the probability of occurrence of specific SLD values (e.g., the probability of SLDs less than 5 m or the probability of SLDs exceeding 70 m). We determined these values at each grid point based on the 37 years of SODA data and then created SLD threshold probability maps. The specific thresholds were chosen based on the operational implications of SLD and were for up to six SLD ranges: (1) less than or equal to 5 m; (2) greater than 5 m and less than 25 m; (3) greater than 25 m and less than 46 m; (4) greater than 46 m and less than or equal to 70 m; (5) greater than 70 m and less than or equal to 112 m; and (6) greater than 112 m. We feel that such probabilistic information is operationally relevant for USW planners when long-range decisions are being made about platform assignments, sensor placement, and operational area (OPAREA) selection.

3. Predictands

The main predictand for our long-range forecasts was area averaged SLD for specific months and regions of interest based on operational or tactical significance in USW planning and/or scientific assessment. The main factors we considered in selecting the regions were:

- (1) The need for long-range forecast support in the region
- (2) The operational and/or tactical significance of the region
- (3) The spatial patterns of environmental variability in and near the region
- (4) The long-term mean SLD value in and near the region

The predictand is the area averaged value for a specified region. Thus, we chose predictand regions for which the long term mean SLDs and SLD standard deviations were similar at all grid points within the region. This was balanced by a need to keep the predictand region small enough that spatial smoothing was minimized and the resulting SLD forecast would be useful in operational planning. For our study, we evaluated multiple predictand regions. Specific results for two of these predictand regions are presented and discussed in Chapter III.

4. Correlations and Teleconnections

To identify potential long lead predictors for the predictands, we used the NOAA/ESRL mapping and analysis tools, to correlate time series of each predictand (e.g., SLD in a portion of the East China Sea) with other environmental variables (e.g., winds, SST, temperature, geopotential heights) on a global scale, with the potential predictors leading the predictand by zero to four months. Significant correlations occurring on global scales are evidence of long distance dynamical interactions within the climate system. Such interactions are called teleconnections. Our correlations were calculated using monthly means from 1970–2006. Correlations greater than $+\text{-} 0.314$ were considered statistically significant at the 95% confidence interval, based on the standard normal distribution of a two-tailed test (Wilks 2006). In general, the strongest correlations at multiple month lead times were between SLD in the WNP and SST in the equatorial and southern tropical Pacific (correlation magnitudes exceeding 0.5).

5. Predictors

In our study, we defined a predictor as a variable with significant long lead correlations with a predictand. The predictors represent area averaged values for a region. Thus, we chose predictor regions for which the correlations with the predictor were strong and relatively similar at all grid points within the regions. We also considered the dynamical basis for the correlations when selecting

predictors, preferring predictors for which plausible dynamical explanations for the correlations could be identified (e.g., explanations based on low frequency wave mechanisms that allow climate variations in the tropical Pacific to influence the WNP).

We evaluated multiple variables as potential predictors (e.g., surface air temperature, surface wind, geopotential height, sea surface temperature) and found many for which significant correlations with SLD in the WNP existed. We selected Pacific SST predictors for the two SLD predictand regions presented in Chapter III because its correlations with WNP SLD were stronger and more significant at long lead times than those for other potential predictors.

6. Predictor and Predictand Time series

Once the main SLD predictands and corresponding SST predictors were chosen, we analyzed their time series to identify intraseasonal to decadal patterns of variability in the predictors and predictands, and in their correlations with each other. We also used the time series to identify extreme events for use in conditional composite analyses and multi-year trends that might influence the selection of long-range forecasting methods.

7. Tercile Matching Forecast Method

For this study, we used a simple tercile matching method to conduct multi-year hindcasts and assess the potential value of the predictor-predictand relationships in long-range forecasting. The method is based on grouping the 37 years of predictand and predictor values into above normal (AN), normal (NN), and below normal (BN) terciles, with each tercile representing approximately 13 years. The sign of the predictor-predictand correlation was used to determine how to use the predictor to produce a LRF of the predictand values for any given year. For example, we identified a positive correlation between equatorial-dateline Pacific SST in July and ECS SLD in October based on data from 1970–2006. Thus, we used the occurrence of AN SST in July 1997 to produce a hindcast of AN SLD in the ECS in October 1997. Similarly, BN (NN) SST in July

of a given year was used to produce a hindcast of BN (NN) in October of that year. Through this approach, we developed simple deterministic hindcasts of the AN, NN, and BN October SLD for all years 1970–2006. We then verified those hindcasts by comparing them to the actual SLD. The results of the verification allowed us to assess the viability of the predictor-predictand pairs and the potential benefits of applying more sophisticated long-range forecasting methods.

The hindcast verification was done using standard three by three contingency table methods (cf. Wilks 2006). We determined the number of hits, misses, false alarms (FA), and correct rejections (CR) for AN, NN, and BN predictor conditions that occurred at lead times of zero to four months. For example, in Table 2, the value in the hit cell of the table represents the number of years in which AN SST occurred in August and AN SLD occurred in the following October. The miss value in Table 2 represents the total number of cases in which AN SLD did occur in October, but was not hindcasted due to conditions other than AN SST in the preceding August. The FA value represents the total number of cases in which AN SST in the preceding August led to a hindcast of AN SLD but AN SLD did not occur. The CR value represents the total number of cases in which conditions other than AN SST in the preceding August led to a hindcast of conditions other than AN SLD in October, and AN SLD did not occur.

Table 2. Schematic contingency table for hindcasts of AN SLD in October using SST in August as the predictor and assuming a positive correlation between the predictor and predictand. Note that hit, miss, FA, and CR values would be different for a different predictor and/or different predictand (e.g., BN SST predictor and AN SLD predictand).

Contingency Table for Predictions of AN SLD in October Based on SST Conditions in August			
		Predictor	
Predictand	<u>AN SST</u>	NN SST	BN SST
<u>AN SLD</u>	<i>Hit</i>	<i>Miss</i>	<i>Miss</i>
NN SLD	<i>False Alarm</i>	<i>Correct Rejection</i>	<i>Correct Rejection</i>
BN SLD	<i>False Alarm</i>	<i>Correct Rejection</i>	<i>Correct Rejection</i>

From our contingency table results, we calculated several verification metrics, including: percent correct (PC), false alarm rate (FAR), probability of detection (POD), and Heidke skill score (HSS). See Wilks (2006) for more information regarding these metrics (e.g., how they are calculated, their strengths, and weaknesses). We chose to work with several metrics because individual metrics do not generally provide enough information to assess a forecasting method. Larger (smaller) values of PC, POD, and HSS indicate more skillful forecasts. The HSS is based on a scale of minus one to plus one, with the best HSS equal to one. A HSS of zero indicates that the forecast has no skill with respect to the reference forecast (in this case the LTM), and a HSS less than zero indicates that the forecast has less skill than the reference forecast

The following metrics criteria were used to determine the viability of each predictor-predictand pair:

- (1) Percent correct (hits + correct rejections) greater than 50 percent
- (2) POD equal to or greater than FAR
- (3) HSS values greater than 0.3

If all three criteria were met, we assumed the predictor-predictand pair was viable and used it in the composite analysis forecast (CAF) process to develop long lead probabilistic forecasts. If the criteria were not met, we repeated the entire process of developing and assessing predictor-predictand pairs.

8. Composite Analysis Forecast

We used the composite analysis forecast (CAF) process to generate probabilistic long-range forecasts based on the conditional probability of a certain event occurring (e.g., the probability of AN SLD conditions occurring in the ECS in October given the occurrence of AN SST conditions in the equatorial-dateline Pacific in August). The CAF process used in our study is an adaptation of the process developed by NOAA (MetEd 2009) and used in previous long-range

forecasting studies by Hanson (2007), Moss (2007), and Crook (2009). The CAF process involves a number of steps, including several of the methods described in prior sections of this chapter (e.g., selection of predictands and predictors).

An additional step is the development of composite analyses based on the observed frequency distribution of the predictand with respect to the predictor for the analysis period, 1970–2006 in our case. In the original CAF process, developed by NOAA, the predictor-predictand relationship is simultaneous (i.e., the predictor does not lead or lag the predictand) and the predictor value is a prediction of the predictor variable at the valid time. For example, a prediction of October SST issued in August is used, along with the simultaneous predictor-predictand relationship for October, to produce a LRF for October that is issued in August. This works well if the predictor is a variable for which relatively skillful LRFs are available (e.g., LRFs of Nino 3.4 SST available from CPC and other operational climate centers). However, our predictors are carefully selected to provide the best correlations with the predictands. This means that, in general, there will not be credible LRFs of the predictors available from other sources (e.g., CPC) or that LRFs of the predictors have to be developed. To overcome these complications, we modified the CAF process so that our predictor-predictand relationships are lagged (predictor leading predictand by one or more months) and our predictors are analyzed values for the time that the LRF of the predictand is issued. For example, we use analyzed SST for August as the predictor for SLD in the following October.

To determine whether the results of our composite analysis distributions were statistically significant, we performed a risk analysis using the hypergeometric distribution method. For our study, we evaluated the statistical significance of our analysis distributions at a 90 percent confidence level (10 percent significance). If, for example, the number of AN, NN, or BN SLD occurrences during AN (warm), NN (normal), or BN (cool) SST conditions at our predictor location were statistically significant, then the SLD predictand and SST

predictor relationship was considered statistically significant and very unlikely to be due to chance. See Wilks (2006) for further information on geometric distribution methods.

If our composite analysis results showed a statistically significant relationship, then that relationship was used to develop a long-range probabilistic forecast using a modified form of the NOAA CAF equations. Figure 13 shows the three equations used to determine the forecast probability for observed SLD in the predictand region to be in the AN, NN, or BN category. In these equations, the P values on the left hand sides of the equations represents the probability of AN, NN, and BN predictand conditions occurring, with the predictand condition being indicated by the subscript (e.g., AN SLD). The P values on the right hand side of the equations represent conditional probabilities, with the subscript indicating the condition (e.g., AN SST) and the superscript indicating the variable for which the probability is being determined (SLD in this case). The full LRF is based on all three equations—that is, on a set of three probabilities for the three predictand states (AN, NN, and BN).

$$P_{AN[SLD]} = P_{AN[SST]}^{AN[SLD]} x P_{AN[SST]} + P_{NN[SST]}^{AN[SLD]} x P_{NN[SST]} + P_{BN[SST]}^{AN[SLD]} x P_{BN[SST]}$$

$$P_{NN[SLD]} = P_{AN[SST]}^{NN[SLD]} x P_{AN[SST]} + P_{NN[SST]}^{NN[SLD]} x P_{NN[SST]} + P_{BN[SST]}^{NN[SLD]} x P_{BN[SST]}$$

$$P_{BN[SLD]} = P_{AN[SST]}^{BN[SLD]} x P_{AN[SST]} + P_{NN[SST]}^{BN[SLD]} x P_{NN[SST]} + P_{BN[SST]}^{BN[SLD]} x P_{BN[SST]}$$

Figure 13. Equations from the original NOAA CAF process used to calculate long-range forecasts of SLD in a predictand region using SST in a specified predictor region. Adapted from (MetEd), May 2009.

The equations in Figure 13 include all three predictand categories and all three predictor categories as defined by the original NOAA CAF process. For our study, and a prior study by Crook (2009), analyzed predictor (e.g., SST) conditions were used versus probabilistic predictions of our predictor. To adapt

the original CAF equations for our study, we used a binary “0” or “1” for predictor probabilities, with “1” representing the probability of the actual analyzed SST condition. Figure 14 shows an example of what the modified CAF equations would look like for a case in which the analyzed predictor condition was AN SST. The resulting long-range probabilistic forecast is constructed from the probabilities derived from each equation in Figure 14 yielding a probability of AN, NN, and BN conditions occurring for a specified predictand (e.g., SLD in October for the East China Sea), given an actual analyses of the predictor (e.g., July SST in the equatorial-dateline Pacific). The sum of each AN, NN, and BN probability will always equal 100 percent. Ideal results would weight one probability greater than the others, for example, a probabilistic forecast showing a 15 percent probability of BN SLD, a 20 percent probability of NN SLD, and a 65 percent probability of AN SLD for a given month. However, it is possible for the forecast to show nearly identical probabilities for each predictand category (e.g., 33 percent probability of AN, NN, and BN SLD), meaning that chances for each SLD occurrence are equally likely.

$$P_{AN[SLD]} = P_{AN[SST]}^{AN[SLD]} x P_{AN[SST]}$$

$$P_{NN[SLD]} = P_{AN[SST]}^{NN[SLD]} x P_{AN[SST]}$$

$$P_{BN[SLD]} = P_{AN[SST]}^{BN[SLD]} x P_{AN[SST]}$$

Figure 14. Equations used in modified CAF process to calculate long-range forecasts of SLD in a predictand region using analyzed AN SST predictor conditions.

It is important to note that if the composite analysis results do not show a statistically significant relationship between the predictor and predictand, a probabilistic forecast cannot be generated using the aforementioned modified CAF equations. For more information on the NOAA CAF method and its

application in developing long-range probabilistic forecast products for Iraq and Afghanistan, see Hanson (2007), Moss (2007), and Crook (2009).

9. Conditional Composite Climatologies

We also used conditional composite climatologies to generate long-range climate support products for USW planners and decision makers. If a probabilistic forecast was generated using the CAF process, then AN, NN, and BN predictor periods were used to create conditional mean and conditional environmental threshold probability maps for the predictand. For example, if a probabilistic forecast was generated for October using August SST as a predictor, then the AN, NN, and BN years for SST in August were used to create conditional mean and conditional environmental threshold probability maps of SLD in October. Similar maps based just on the AN, NN, and BN periods for the predictand were also generated. These maps describe the predictand spatial patterns in the predictand region and in surrounding areas that are associated with the LRFs of the predictands. These maps provide a spatial context for the LRFs and help make the LRFs more operationally relevant.

E. SUMMARY OF CLIMATE ANALYSIS AND LONG-RANGE FORECAST METHODOLOGY

Figure 15 is a schematic of the process used in this thesis to analyze climate variations and generate long-range forecasting support products for USW operations in the WNP. This process uses state of the science oceanic and atmospheric reanalysis data sets, and advanced climate analysis and forecasting methods, to develop deterministic and probabilistic long-range forecasts of sonic layer depth in specific regions within the WNP. While this process was developed using sonic layer depth as the operational variable of interest, it can also be applied to other USW variables of interest (e.g., ILG, BLG, COF). Similarly, it can also be applied to other areas of interest besides the WNP.

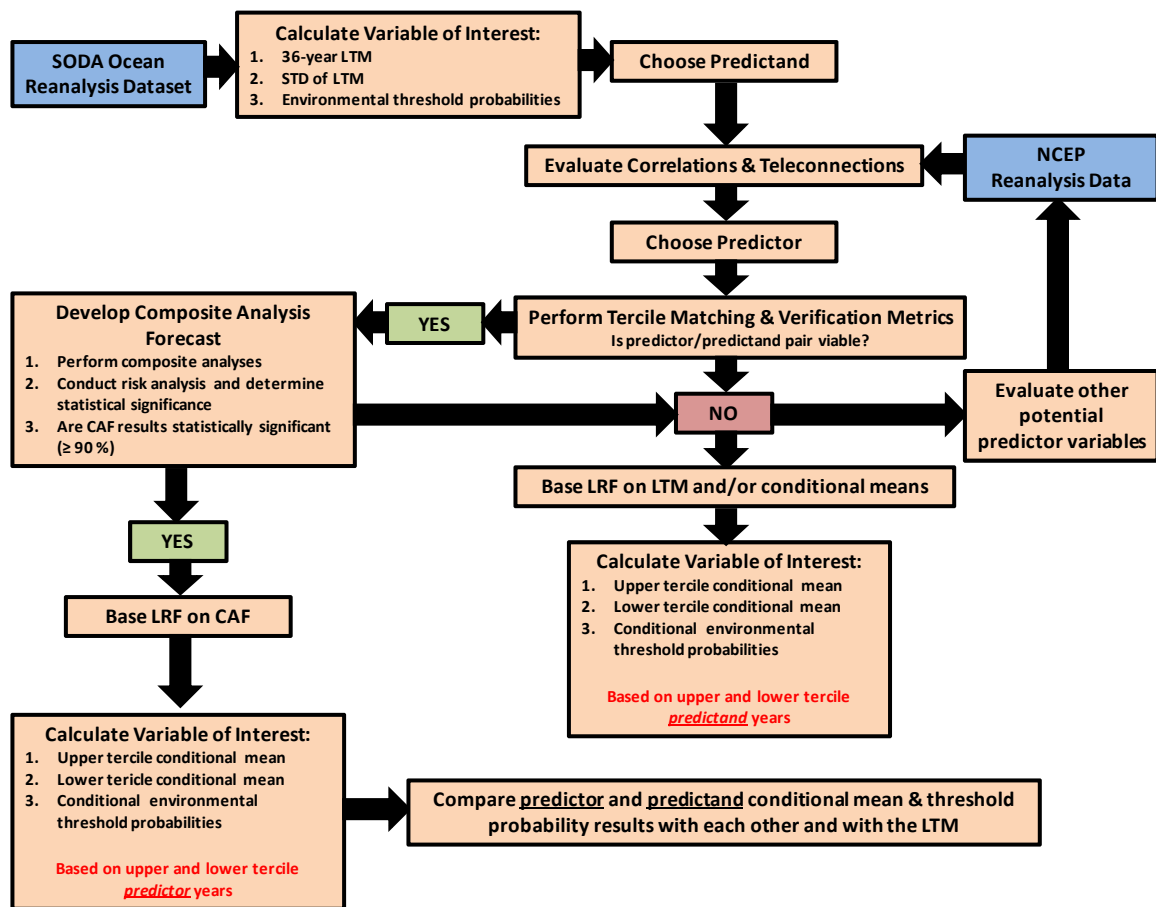


Figure 15. Flow chart showing main data sets and methods used to conduct climate analyses and long-range forecasting for this study.

III. RESULTS

A. SEASONAL VARIATIONS IN THE WNP

1. Winter

In the winter season, a strong surface high pressure system, the Asian High, develops over much of central Asia. Anticyclonic winds associated with this region of high pressure produce northerly and northeasterly monsoon winds, and cold, dry air advection, over the surface of the East Asian marginal seas. These winds promote net heat fluxes from the ocean and mixing within the upper ocean (Open University 2001), leading to deeper SLDs than at other times of the year. Figure 16 shows the LTM SLD and the standard deviation of SLD in the WNP for January. In general, the shallowest SLDs and lowest SLD variability occur in the tropical portions of the WNP, consistent with weaker and more persistent surface winds, and lower net heat fluxes from the ocean, in the tropics than in the higher latitudes (Open University 2001). The deepest SLD and the greatest SLD variability occur in the northern Sea of Japan, and north and east of Hokkaido. The Kuroshio region east of the East China Sea, and south and east of Japan is an area of relatively deep SLD (compare Figures 16a and 17). However, the Kuroshio is an area of relatively low variability in SLD, except in a small region south of southern Honshu where large fluctuations in the location of the Kuroshio occur (compare Figures 16b and 17).

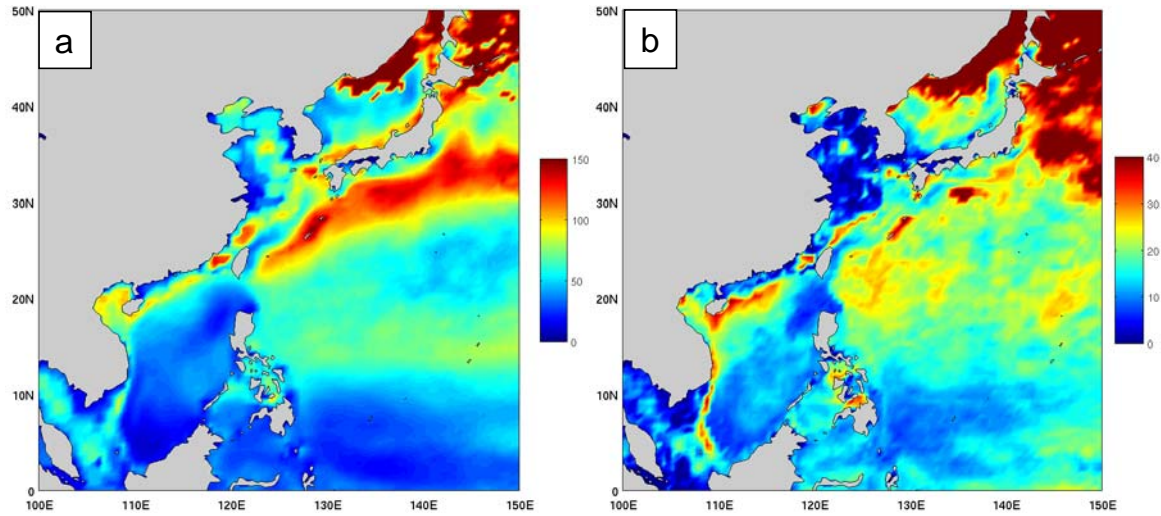


Figure 16. January (a) LTM of SLD (m), and (b) STD of SLD (m) in the WNP. The scales are different for this figure than for the corresponding figures for the other seasons (Figures 18, 19, and 20).

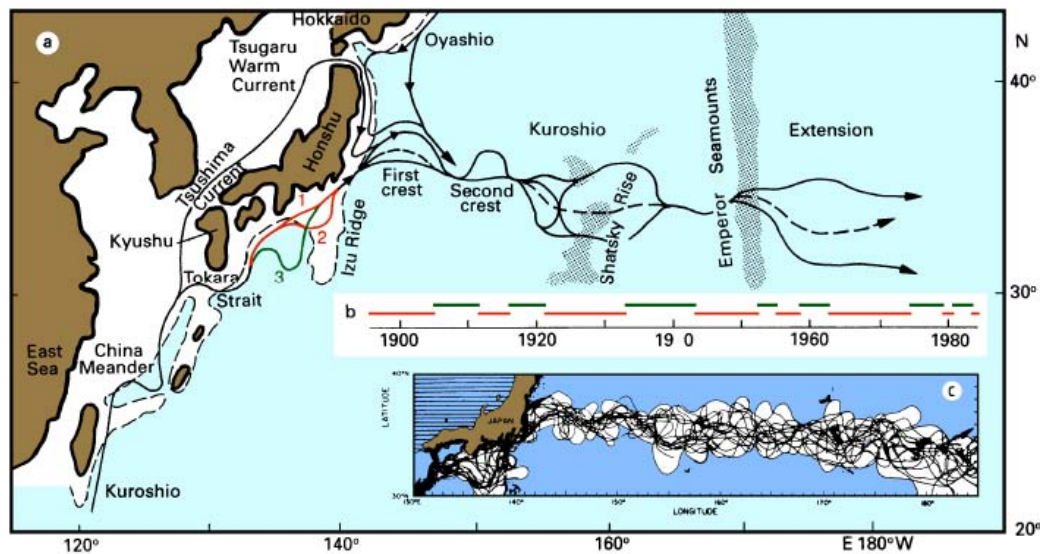


Figure 17. (a) Schematic depiction of the Kuroshio and Oyashio depicted by black lines. The broken black line is the 1000 m contour and indicates the shelf break. As the Kuroshio encounters the Izu Ridge south of Honshu it negotiates along one of three paths depicted in red and green. (b) Time series indicating the annual variability in the Kuroshio paths. (c) Individual Kuroshio paths observed from summer 1976 to 1980. From Tomczak (2003).

2. Spring

In spring, the atmospheric high pressure system over Asia weakens and a transition from winter monsoon to summer monsoon conditions occur in the WNP region. Surface wind speeds over the marginal seas of the WNP tend to be lower than in winter. Figure 18 shows the LTM SLD and standard deviation of SLD for April. SLDs in the Kuroshio are deeper than in most other parts of the WNP but shallower than in the winter, consistent with the weakening of the surface winds. The relatively deep SLD at about 10–15N is an indication of the impacts of the trade winds. These impacts are more evident in the April figures than in those for January; although this is in part a result of the different scaling used in the figures for the two months (compare Figures 16 and 18).

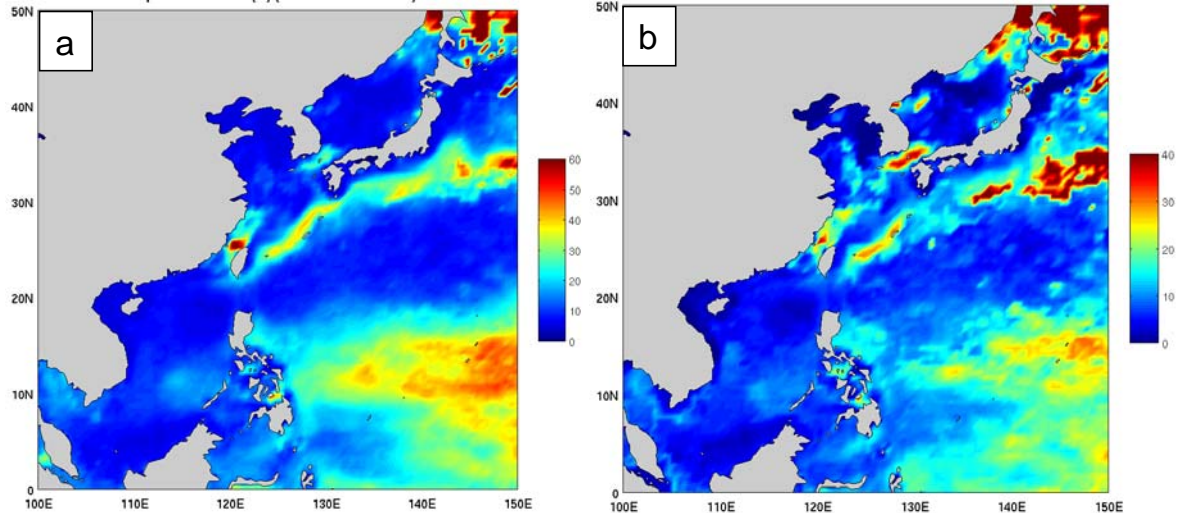


Figure 18. April (a) LTM of SLD (m), and (b) STD of SLD (m) in the WNP. The scales are different for this figure than for the corresponding figures for January (Figure 16).

3. Summer

In the summer, warming of the Eurasian land mass results in low pressures in the lower troposphere over Asia, while high pressure prevails over the subtropical southern Indian Ocean, and North and South Pacific Ocean. This pressure difference leads to the onset of southwesterly and easterly surface winds over much of the tropical and marginal sea regions of the WNP. These

winds enhance mixing of the upper ocean, especially in the South China Sea, Philippine Sea, and western equatorial Pacific. The impacts of these winds are evident in the LTM SLD and the standard deviation of SLD for July (Figure 19), with SLD variations being largest in the tropical portions of the WNP. However, the July SLD and SLD variations are much smaller than those in January. This is most likely due to differences in the net heat fluxes to the ocean in the WNP, which tend to be positive in July but negative in January (Open University 2001). These heat fluxes tend to produce negative (positive) sound speed gradients with depth and shallow (deep) SLDs in July (January). This means that in July (January), wind forced turbulent mixing tends to force the sound speed gradient from negative to neutral (negative to even more negative). Thus, the July winds must work against buoyancy forces and are not able to produce such deep SLDs as winds with similar speeds in January. Note also that in July there is relatively little evidence of the Kuroshio in the LTM SLD or SLD standard deviation, unlike the situations in January, April, and October (compare Figures 16, 18–20). This is consistent with the relatively large positive net heat fluxes to the ocean in the Kuroshio region in July, leading to very shallow SLDs (Open University 2001).

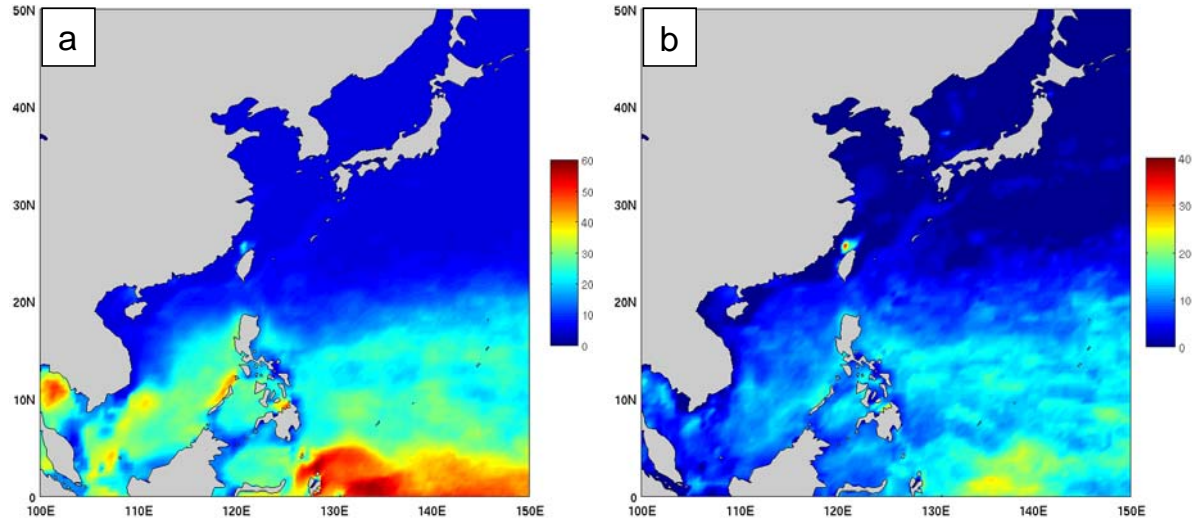


Figure 19. July (a) LTM of SLD (m), and (b) STD of SLD (m) in the WNP. The scales are different for this figure than for the corresponding figures for January (Figure 16).

4. Fall

In fall, the Eurasian land mass begins to cool and conditions in the WNP region begin to shift back toward those of the winter monsoon regime. Figure 20 shows the LTM SLD and the standard deviation of SLD for October. Note the overall similarities between April and October; the two transition seasons (compare Figures 18 and 20). The Kuroshio is evident in the SLD and somewhat evident in the SLD variations.

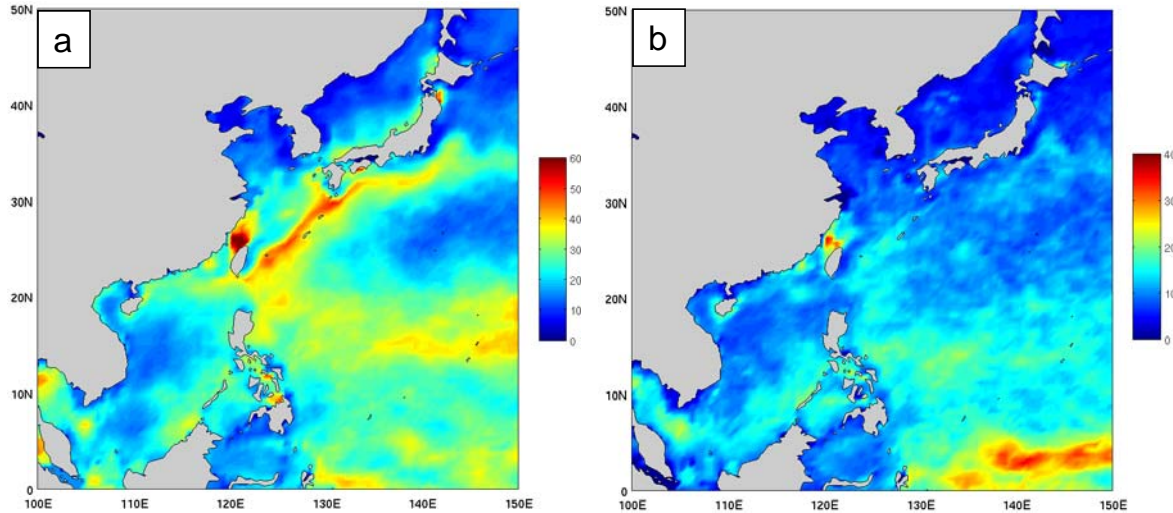


Figure 20. October (a) LTM of SLD (m), and STD of SLD (m) in the WNP. The scales are different for this figure than for the corresponding figures for January (Figure 16).

B. ENVIRONMENTAL FORECAST RESULTS BY REGION

1. October East China Sea Region

The East China Sea (ECS) region has a significant amount of upper ocean variability associated with seasonal climate variations (see Figures 16, 18–20). For this reason, and for its strategic significance to the U.S. military, we chose multiple predictand regions within the ECS to formulate a process for developing long-range USW support products. The month of October was chosen in order to compare our results with those from Turek (2008). Initial analysis of October long term mean sonic layer depth and the standard deviation of sonic layer depth (see Figure 20), enabled us to better understand the patterns

(e.g., high SLD associated with Kuroshio region) and physical processes (e.g., strong northeasterly winds) which drive changes in sonic layer depth for this region. Following the process outlined in Chapter II (see Figure 15) we created environmental threshold probabilities for the WNP for the month of October based on a 37-year record (Figure 21). Environmental threshold probabilities may be used by military planners and decision makers to identify positive and negative conditions for military operations. The environmental threshold probabilities for the Kuroshio region provide an example of what threshold probabilities reveal and how they can be used operationally. Figure 21 shows that in most of the Kuroshio region in October, there is a very low probability of experiencing SLDs less than 25 m or greater than 70 m, but a high probability of SLDs between 25 and 70 m. In addition, Figure 21 shows nearby regions in which other SLD values are probable—for example, regions adjacent to the Kuroshio in which shallower or deeper SLDs are probable. This type of information is very relevant for planning USW operations and allows decision makers to quickly determine, in a probabilistic way, how the operational environment can vary over small spatial scales (e.g., along the edge of the Kuroshio). This information can be crucial in determining platform assignment and sensor placement when conducting USW operations.

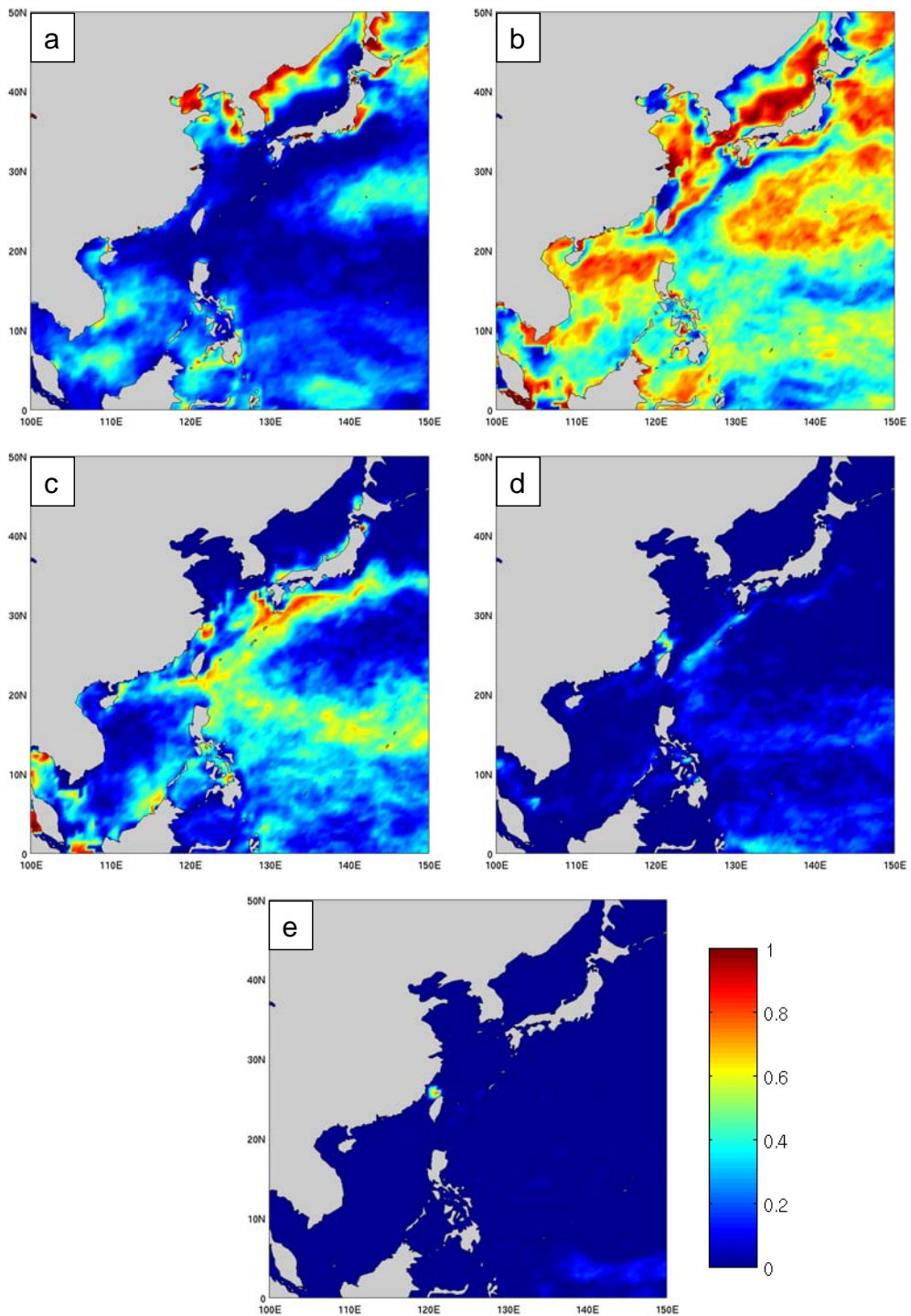


Figure 21. October SLD environmental threshold probabilities. Probability of SLD: (a) less than or equal to 5 meters; (b) greater than 5 meters and less than or equal to 25 meters; (c) greater than 25 meters and less than or equal to 46 meters; (d) greater than 46 meters and less than or equal to 70 meters; and (e) greater than 70 meters.

From our analysis of the LTM and standard deviation of sonic layer depth, we chose three potential predictand regions (Figure 22) to develop a long-range probabilistic forecast product. The first region is outlined by the red box in Figure 22 and is identical to the focus region used in Turek (2008). The second region is outlined in black in Figure 22 and was chosen because it encompasses the greatest October LTM SLD values in the Kuroshio region. The third region consisted of the three small blue boxes plus the black box in Figure 22, and was chosen to represent a larger region of the Kuroshio focused on the area of deepest SLD and largest SLD variation during October (Figure 20b). Correlations, hindcasting, and CAF computations were conducted for each potential predictand region as described in Chapter II, sections D3–D8. However, only the results for the third, multi-box predictand, which we refer to as the ECS predictand region, are presented. The results for this region are broadly representative of those for the other two regions.

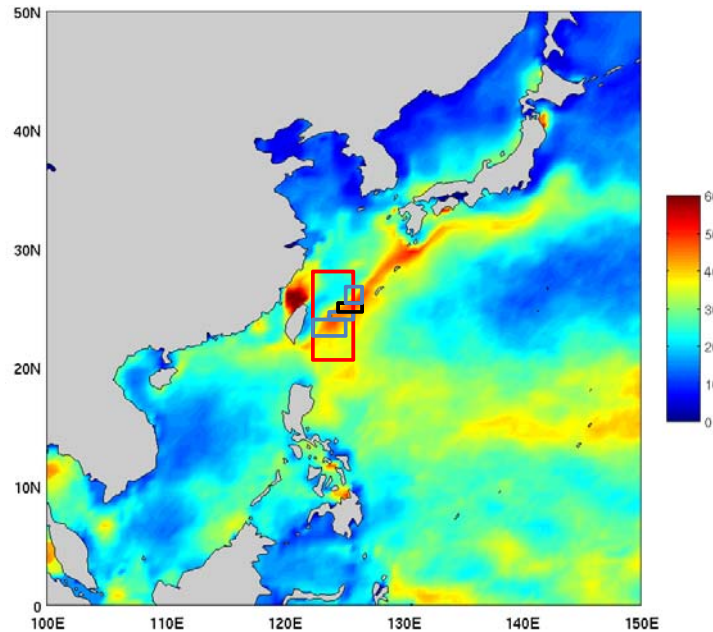


Figure 22. October LTM SLD (m) showing three main October predictand regions used in this study. Large SLD potential predictand region indicated by red box (20° – 28° N, 122° – 126° E). Small SLD potential predictand region indicated by black box (25° – 26° N, 125° – 127.5° E). Multi-region SLD potential predictand region indicated by light blue and black boxes (22° – 24° N, 123° – 126° E, 24° – 25° N, 124° – 127° E, 25° – 26° N, 125° – 127.5° E, 26° – 27° N, 126° – 127.5° E).

We correlated the area average SLD for the October ECS SLD predictand region with global SST to identify potential predictor regions for this SLD predictand. Figure 23 shows the correlations with SST leading the SLD predictand by zero to three months. Figure 23 (panel a) shows a large area of negative correlation at zero lead centered over the predictand region in the western WNP, indicating that, in this region, SST is low when SLD is deep, and vice versa. This negative correlation is pronounced at zero lag but much less evident at one to three months lead. This is expected and indicates that when SST decreases (e.g., cools due to surface heat fluxes and/or strong cold northeasterly winds at the surface causing turbulent mixing), SLD responds relatively quickly and increases (deepens). At all lead times, there is a pronounced pattern of negative correlations in the western tropical south Pacific and positive correlations in the central tropical Pacific, especially along the equator near the dateline. This is strikingly similar to the correlations between ECS surface winds and SST (Figure 8), although the signs are reversed for the two sets of correlations. Thus, Figure 23 extends the findings of Turek (2008) and indicates that tropical Pacific SST variations lead to atmospheric circulation variations in the ECS that then lead to SLD variations, with SST increases (decreases) in the summer being associated with increased (decreased) surface wind speeds and SLD in the ECS in the following October.

The correlation patterns in the Pacific in Figures 8 and 23 are similar in some respects to the SST anomaly patterns associated with El Nino and La Nina events (e.g., the wedge shaped area of positive correlations in the central and east Pacific centered on the equator and bounded by negative correlations to the west; Ford 2000). This suggests that an index of El Nino and La Nina events might be a predictor of ECS winds and SLD. However, our results and those of Ramsaur (2009) (not shown) indicate that such indices are not as well correlated as other tropical Pacific SST predictors.

The correlations shown in Figure 23 helped us identify as a potential predictor of ECS SLD the SST along the equator just west of the dateline in the region bounded by 5°N – 5°S , 160° – 185°E . This region has consistently strong positive correlations at zero to three month lead times. This region is also the western half of the NINO 4.0 region.

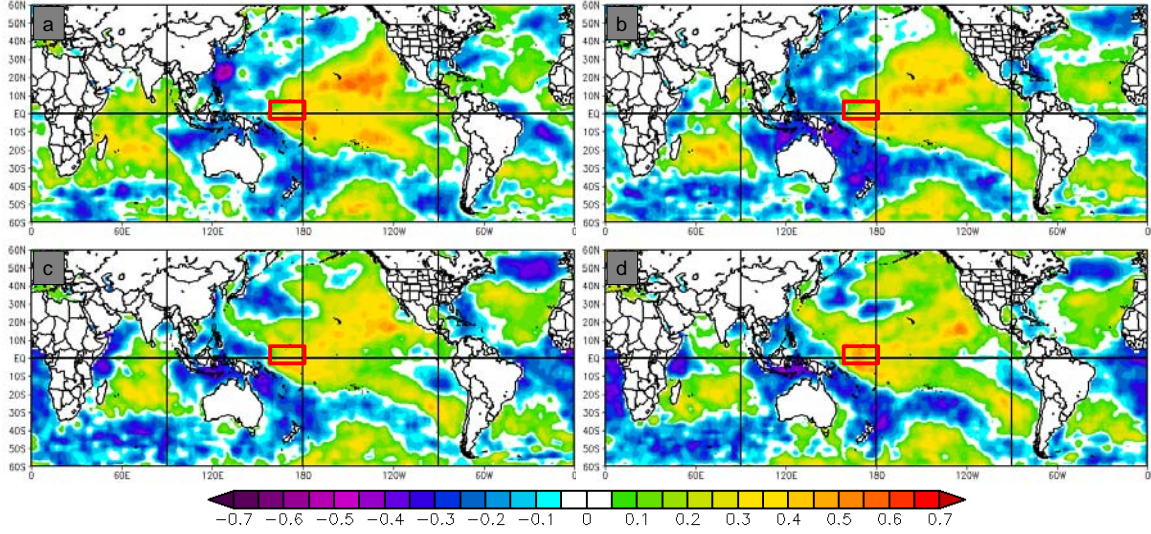


Figure 23. Correlations between the October ECS SLD predictand and SST in: (a) October; (b) September; (c) August; and (d) July, based on data from 1970–2006. Note the strong positive correlations in the central and eastern tropical Pacific. We chose the area of high positive correlations between 5°N – 5°S , 160° – 185°E (red box) as our potential predictor. For the October SLD predictand.

To better assess the ECS SLD predictand and the potential equatorial-dateline Pacific SST predictor (e.g., to identify their interannual and longer term variations, and potential events for compositing), we created time series showing the predictor and predictand values during the study period (Figure 24). As expected, the predictor and predictand generally vary in phase with each other. The time series also provided information on multi-year trends in the predictor and predictand that we used in developing the long-range forecasting process (see discussion of the composite analysis forecasting process later in this section). Figure 24 shows a strong positive correlation between the July and

October SST predictor time series, indicating a high degree of persistence in the predictor and a high potential for skillful forecasts of the predictand at lead times of several months.

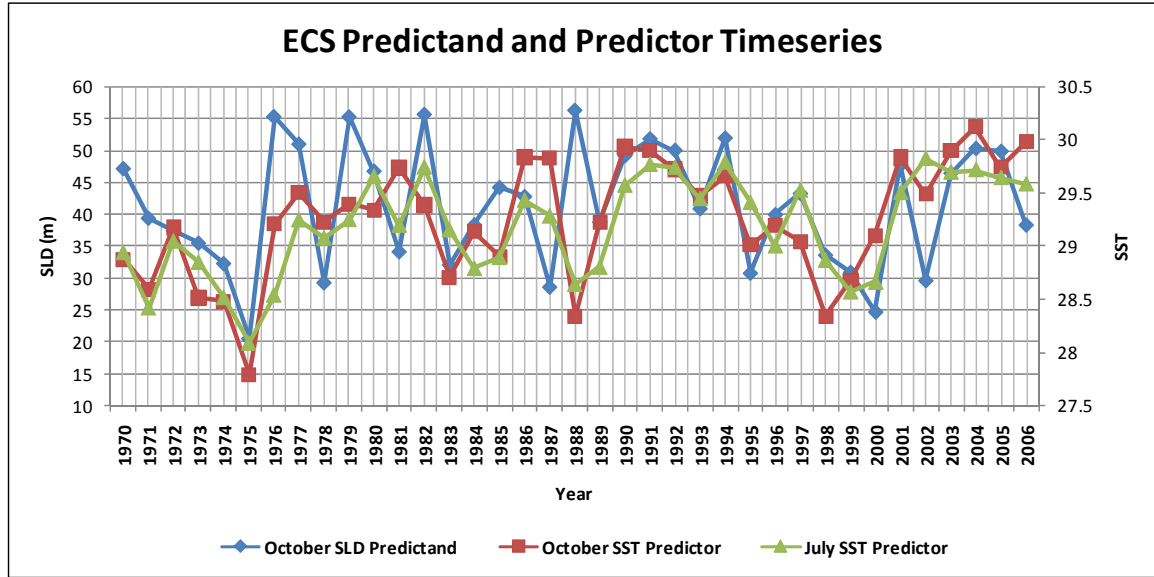


Figure 24. Time series of ECS SLD predictand (blue line), October SST predictor (red line), and July SST predictor (green line) for 1970–2006.

Based on our correlation results, we applied the tercile matching method to conduct multi-decadal hindcasts and assess the viability of our selected predictor-predictand pair. In Table 3, columns A, B, C, and D represent the number of hits, false alarms, misses, and correct rejections calculated for each predictand condition (e.g., AN SLD, BN SLD, and NN SLD) at zero, one, two, and three month lead times. These values were used to calculate four verification metrics, percent correct (%Corr), false alarm rate (FARate), probability of detection (POD), and Heidke skill score (HSS). Based on a set of criteria described in Chapter II, section D7, we used these metrics to determine whether we would use our predictand-predictor pair to create a probabilistic long-range forecast. The results for the equatorial-dateline SST predictor and the October ECS SLD predictand (Table 3) show that for many of the predictand terciles and lead times our verification metrics criteria were met (e.g., POD greater than 0.50,

POD greater than FARate, HSS of 0.3 or greater). These results gave us confidence that this predictor-predictand pair was viable, and could be used in the CAF process to generate a skillful long lead probabilistic forecast.

Table 3. Contingency table results and verification metrics from hindcasts generated using the tercile matching forecast method. Hindcasts of 1970–2006 October ECS SLD predictand based on equatorial-dateline SST predictor, with predictor leading by zero to three months. Columns A, B, C, and D represent the number of hits, false alarms, misses, and correct rejections respectively for AN, BN, and NN SLD values. See Chapter II, section D7, for details on contingency table and verification metrics.

	A	B	C	D	VERIFICATION METRICS			
	Hits	FA	Misses	Corr. Rej.	% Corr	FA Rate	POD	HSS
OCT Equatorial-dateline SST Predictor Index VS. ECS SLD Predictand Index								
AN SLD	7	5	5	20	0.730	0.417	0.583	0.425
BN SLD	7	5	5	20	0.730	0.417	0.583	0.425
NN SLD	6	7	7	17	0.622	0.538	0.462	0.248
SEP Equatorial-dateline SST Predictor Index VS. ECS SLD Predictand Index								
AN SLD	7	5	5	20	0.730	0.417	0.583	0.425
BN SLD	6	6	6	19	0.676	0.500	0.500	0.320
NN SLD	5	8	8	16	0.568	0.615	0.385	0.154
AUG Equatorial-dateline SST Predictor Index VS. ECS SLD Predictand Index								
AN SLD	7	5	5	20	0.730	0.417	0.583	0.425
BN SLD	5	7	7	18	0.622	0.583	0.417	0.218
NN SLD	4	9	9	15	0.514	0.692	0.308	0.063
JUL Equatorial-dateline SST Predictor Index VS. ECS SLD Predictand Index								
AN SLD	7	5	5	20	0.730	0.417	0.583	0.425
BN SLD	6	6	6	19	0.676	0.500	0.500	0.320
NN SLD	5	8	8	16	0.568	0.615	0.385	0.154

Using our ECS SLD predictand and equatorial-dateline SST predictor we developed composite analysis forecasts for the East China Sea in October using the CAF process outlined in Chapter II, section D8. Figure 25 (panel a) shows the composite analysis for ECS SLD in October and equatorial-dateline SST in July. The statistically significant results, outlined in black, are for AN SST and AN SLD, and BN SST and AN SLD. In Figure 25 (panel a) we also see a general pattern indicating highest (lowest) probability of AN SLD conditions when there are AN SST (BN SST) conditions in the predictor region and highest (lowest)

probability of BN SLD conditions when there are BN SST (AN SST) conditions in the predictor region. This pattern is consistent with the correlation and hindcast results.

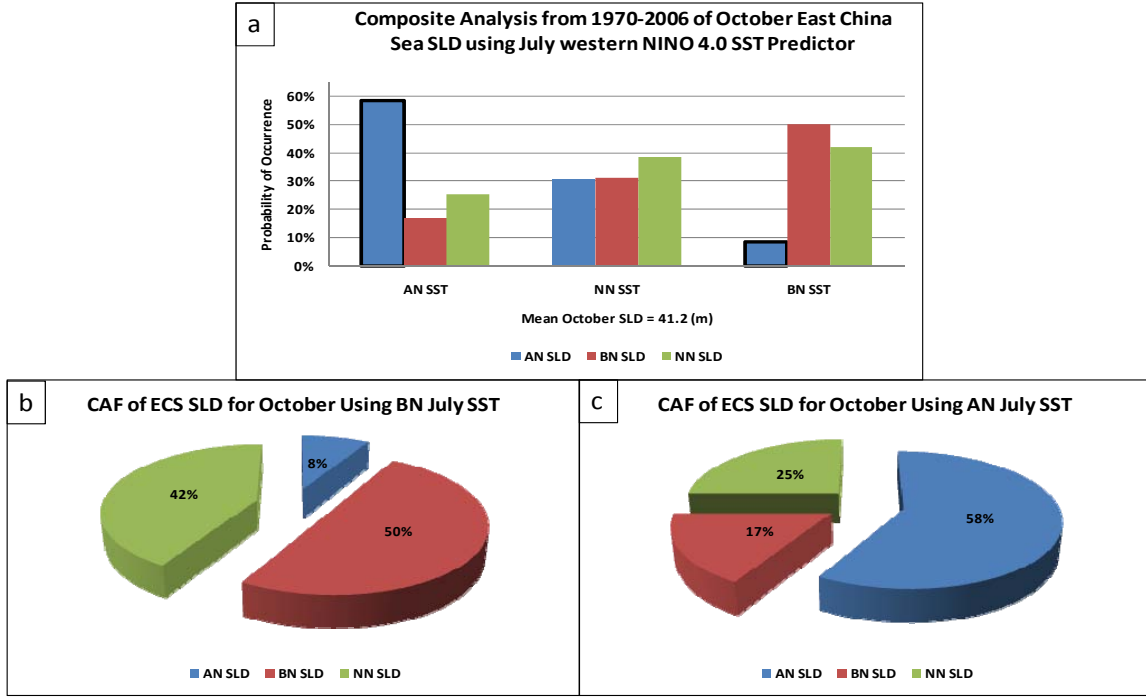


Figure 25. (a) Composite analysis for October SLD in the ECS using the equatorial-dateline SST predictor in July. Statistically significant results are outlined in black. (b) Corresponding probabilistic long-range hindcast of ECS SLD in October based on BN equatorial-dateline SST predictor in July. (c) Corresponding probabilistic long-range hindcast of ECS SLD in October based on AN equatorial-dateline SST predictor in July. For July 2009, the SST predictor values are AN (see Figure 26). Thus, our CAF prediction of October 2009 ECS SLD based on July 2009 equatorial-dateline SST conditions would be: probability of above normal SLD—58%; probability of near normal SLD—25%; and probability of below normal SLD—17%.

Using statistically significant results from our composite analysis we generated two probabilistic long-range hindcasts of sonic layer depth in the East China Sea for October (see Figure 25 panels b and c). These probabilistic long-range hindcasts indicate that the CAF process may be used to generate skillful long-range forecasts of East China Sea SLD in October using July SST conditions in our equatorial-dateline predictor region

To make a prediction of East China Sea sonic layer depth for October 2009 we determined that July 2009 SST conditions in our predictor region were AN (Figure 26), and applied this information to produce a long-range forecast based on the composite analysis results (Figure 25, panel a). This led to a probabilistic long lead forecast, which would be issued at the end of July 2009, valid for October 2009 that showed a 58 percent probability of AN, 25 percent probability of NN, and 17 percent probability of BN sonic layer depths in the East China Sea based on a mean SLD value of 41 meters.

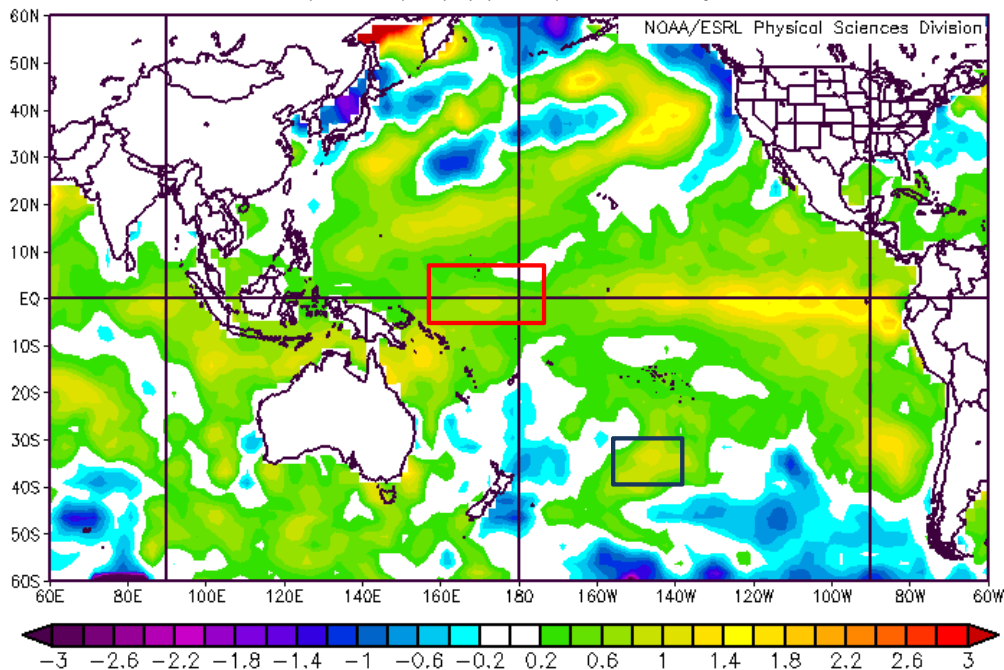


Figure 26. SST anomalies ($^{\circ}\text{C}$) for July 2009. ECS equatorial-dateline SST predictor (red box). NAX south Pacific SST predictor (blue box). Image from (ESRL), July 2009.

We also generated conditional mean and conditional environmental threshold probability composites as additional long lead support products for military planners and decision makers. Conditional mean and conditional environmental threshold probability composites of AN and BN October sonic layer depth in the ECS were calculated using upper and lower tercile July SST predictor years from 1970–2006. These products correspond to what might be issued as a forecast product, since they are based on conditions in the preceding

July. For comparison, we also generated the conditional mean and conditional threshold probability composites of AN and BN October sonic layer depth using upper and lower tercile October SLD predictand years from 1970–2006. These products correspond to what might be issued as part of a verification product, since they are based on conditions during the October valid period. The difference between these two products is a measure of the uncertainty in the long-range forecasts, for example, a measure of the uncertainty in LRFs of AN October SLD based on AN July SST predictor conditions.

Figure 27 shows examples of these products. Notice that upper (lower) tercile composite means of October sonic layer depth using July SST predictor years are very similar to upper (lower) tercile composite means using October SLD predictand years. However, the means based on the October SLD predictand years are more extreme (e.g., panels c and d show deep SLDs in the Kuroshio region northeast of Taiwan, but panel d shows deeper SLDs in that region than panel c). This indicates that the means based on the July SST predictor years include some years that were not among the most extreme years. The differences between the corresponding composite means (a and b, c and d) occur because, while we have shown that SST is a skillful predictor of SLD, it is not the only variable factoring into determination of sonic layer depth in this region. So, while some upper (lower) tercile July SST predictor years are also upper (lower) tercile October SLD predictand years, not every AN (BN) July SST predictor leads to AN (BN) October SLD predictand conditions.

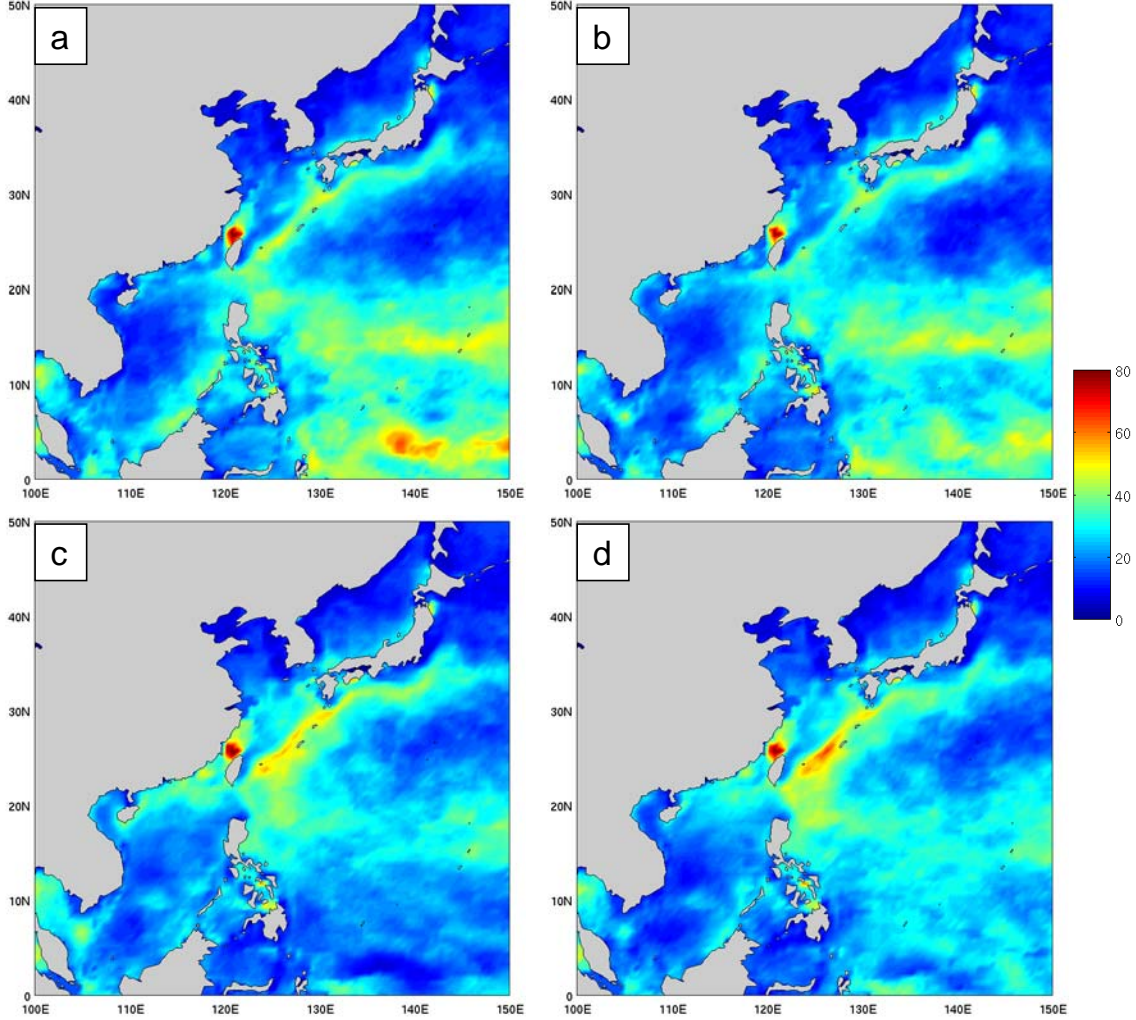


Figure 27. Conditional mean of October SLD based on compositing: (a) lower tercile July SST predictor years; (b) lower tercile October SLD predictand years; (c) upper tercile July SST predictor years; and (d) upper tercile October SLD predictand years.

Figure 29 shows upper tercile conditional environmental threshold probability composites based on AN July SST predictor years and AN October SLD predictand years. These figures only represent upper tercile comparisons, corresponding to our prediction of AN ECS SLD in October 2009 based on AN July 2009 SST predictor conditions. For each of the five threshold comparisons between July SST predictor years and October SLD predictand years in Figures 28 and 29, there is very little difference in the overall probability patterns. This means, for example, that a USW planner could be relatively confident in using

the predicted environmental threshold probabilities valid for October 2009 (Figure 28, panels a and c and Figure 29, panels a, c, and e) issued at the end of July 2009, to determine platform assignments, sensor placement, and for other information on determining the best place to look for a target.

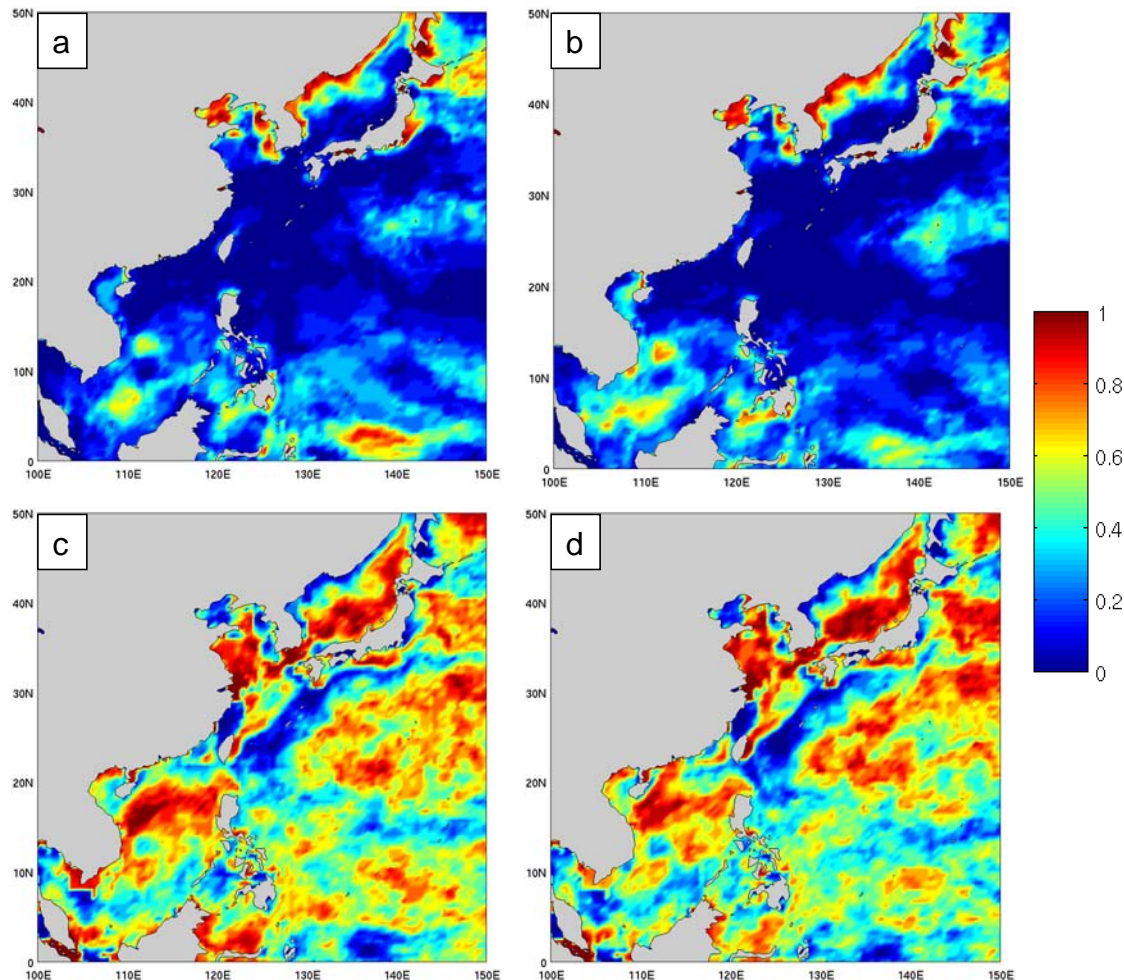


Figure 28. October SLD threshold probabilities based on upper tercile July SST predictor years and upper tercile October SLD predictand years. Probability of SLD: (a) less than or equal to 5 meters using July SST predictor; (b) less than or equal to 5 meters using October SLD predictand; (c) greater than 5 meters and less than or equal to 25 meters using July SST predictor; and (d) greater than 5 meters and less than or equal to 25 meters using October SLD predictand.

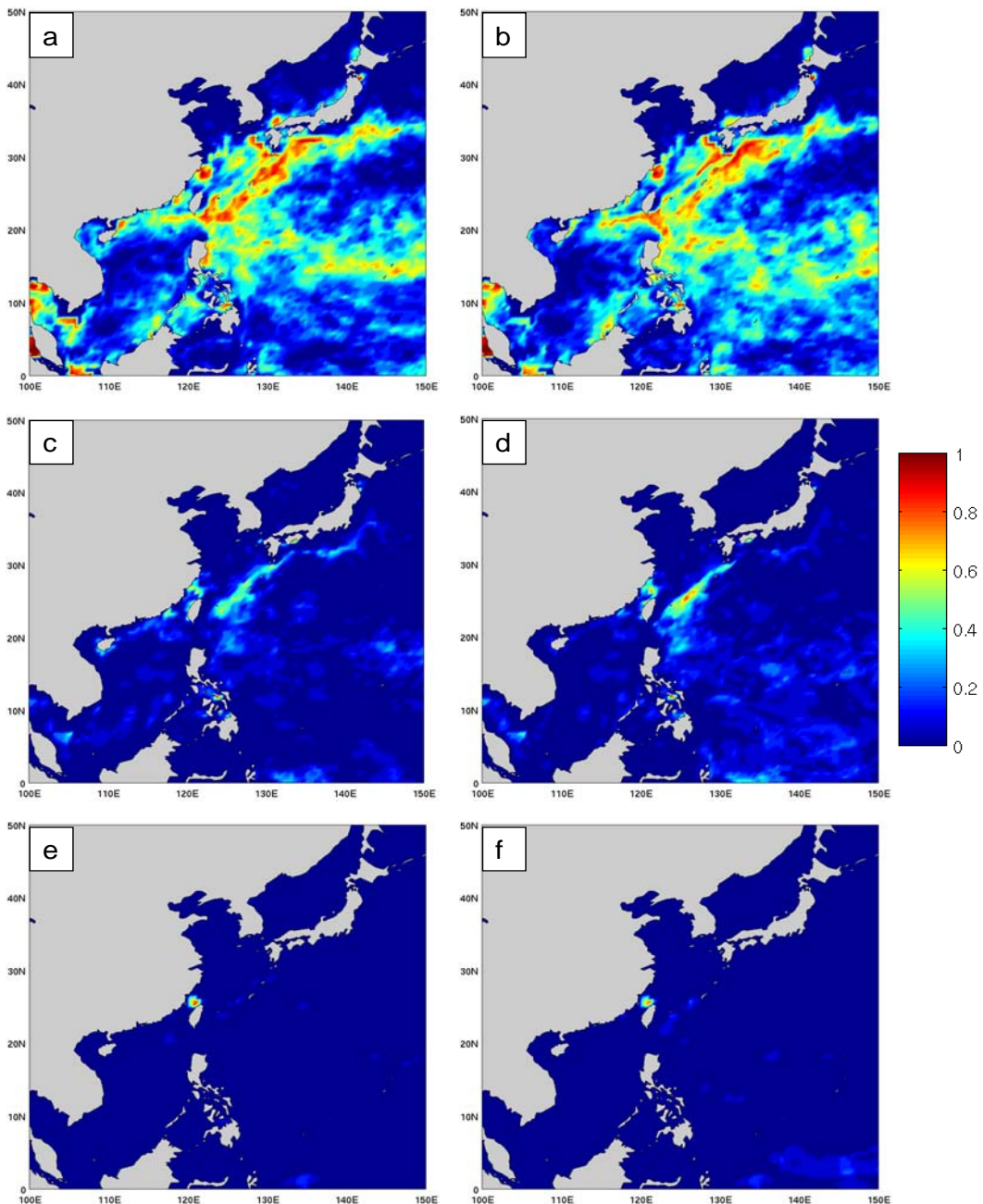


Figure 29. October SLD threshold probabilities based on upper tercile July SST predictor years and upper tercile October SLD predictand years. Probability of SLD: (a) greater than 25 meters and less than or equal to 46 meters using July SST predictor; (b) greater than 25 meters and less than or equal to 46 meters using October SLD predictand; (c) greater than 46 meters and less than or equal to 70 meters using July SST predictor; (d) greater than 46 meters and less than or equal to 70 meters using October predictand; (e) greater than 70 meters using July SST predictor; and (f) greater than 70 meters using October SLD predictand.

2. November ANNUALEX Region

ANNUALEX is a U.S. Navy undersea warfare exercise that occurs every year in the western north Pacific. In 2009, ANNUALEX is scheduled to occur in November, and we chose to use the process outlined in Chapter II to develop long lead support products for USW planners to use in the mid-phase planning aspect of this important naval exercise. Looking at the LTM and standard deviation of SLD in November we see that the Kuroshio is well defined and represented by deep sonic layer depths (Figure 30, panels a and b). This is what we expect during the winter season based on enhanced mixing in the upper ocean due to the northeasterly monsoon wind regime and net surface heat fluxes from the ocean. Sonic layer depths are relatively shallow near the equator where we expect warmer surface waters to cause a negative sound velocity gradient. While LTM sonic layer depth along the equator is close to zero, there is a large amount of variability associated with interannual climate variations (e.g., El Nino and La Nina). This type of information is very valuable to USW planners. For example, an area that has a deep LTM SLD with little or no variability might be an ideal location to plan to conduct operations at long lead times, whereas an area with deep LTM SLD and a lot of variability may not be.

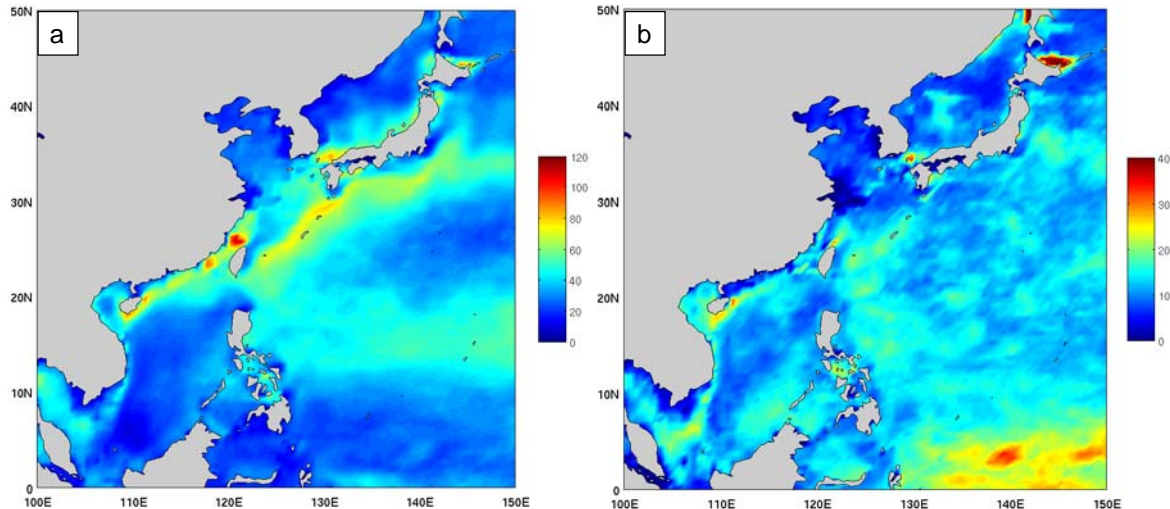


Figure 30. November (a) LTM of SLD (m), and (b) STD of SLD (m) in the WNP. The scales are different for this figure than for the corresponding figures for different months (Figures 16, 18–20).

LTM SLD environmental threshold probabilities were calculated for USW planners to use as long lead planning tools for ANNUALEX 2009 (Figure 31).

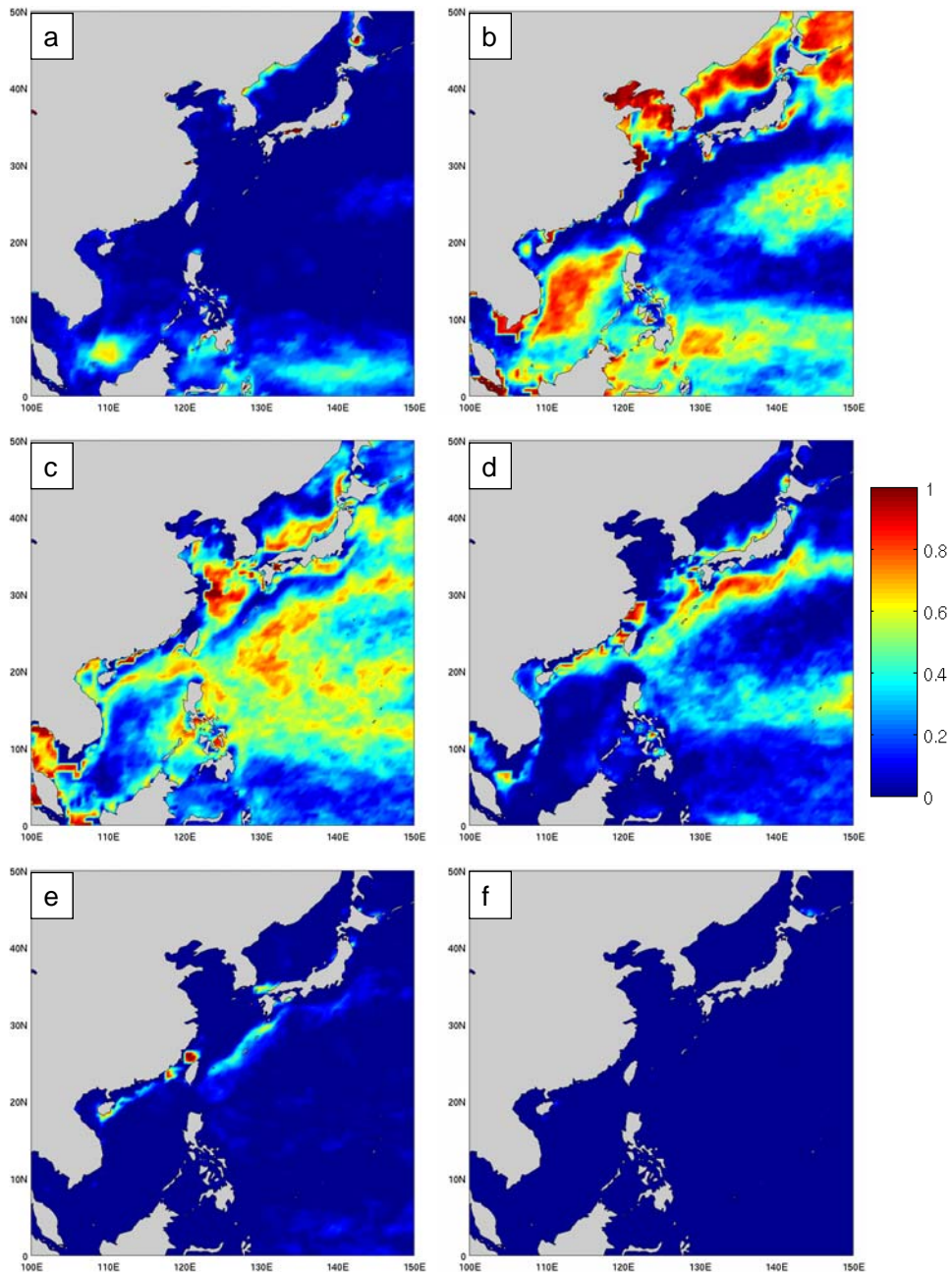


Figure 31. November SLD threshold probabilities showing probability of SLD: (a) less than or equal to 5 meters; (b) greater than 5 meters and less than or equal to 25 meters; (c) greater than 25 meters and less than or equal to 46 meters; (d) greater than 46 meters and less than or equal to 70 meters; (e) greater than 70 meters and less than or equal to 112 meters; and (f) greater than 112 meters. Based on ocean reanalysis data for 1970–2006.

When the exact operating area (OPAREA) for an operation has not been pre-determined, support products such as those shown in Figures 30 and 31 may be useful to planners in establishing an OPAREA or adjusting it based on the expected acoustic environment. However, for many operations and exercises, such as ANNUALEX 2009, the OPAREA is pre-determined at lead times of several months or seasons. In these cases, more focused long lead support products can be developed. Figure 32 shows the November LTM SLD for the WNP with the approximate ANNUALEX OPAREA outlined by the black box. The red and green boxes represent sub-regions within the OPAREA that we chose as potential SLD predictand regions. The entire OPAREA and both sub-regions were evaluated for their long lead forecast potential, since in many cases it is important for USW planners to know how different sub-regions within their OPAREA differ from one another. For example, our LRFs might indicate a 69 percent probability of having AN SLD conditions in the red sub-region, but only a 17 percent probability of AN SLD conditions in the green sub-region.

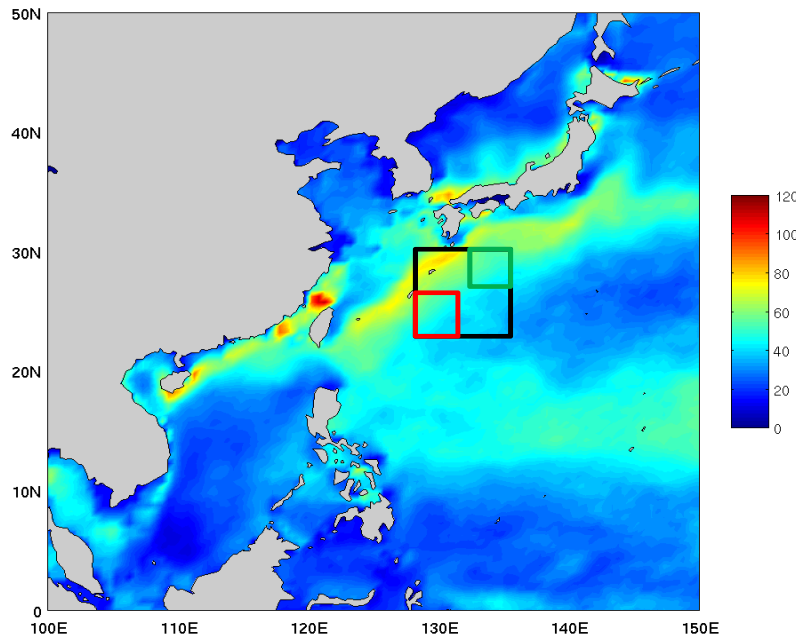


Figure 32. November LTM SLD (m). ANNUALEX OPAREA indicated by black box (24° – 30.5° N, 128.5° – 134.5° E). Red (24° – 27° N, 128.5° – 131° E) and green (28.5° – 30.5° N, 132° – 134.5° E) boxes indicate potential SLD predictand regions within the larger ANNUALEX region.

Using the process outlined in Chapter II, section D3–D8, we developed and evaluated correlations, hindcasts, and CAF-based LRFs for each of our three potential ANNUALEX SLD predictand regions. For brevity, only the results for the red predictand region, which we will now refer to as the November ANNUALEX (NAX) region, are presented.

Figure 33 shows the correlations between area averaged SLD in the NAX predictand region with global SST, with SST leading by zero to four months. The overall patterns are similar to those for October ECS winds and SLD (Figures 8 and 23), and indicate that climate scale variations in SST may induce low frequency atmospheric circulation responses, similar to those associated with El Nino and La Nina events, that affect atmospheric conditions in the WNP. The stronger correlations with the south Pacific SST in July than in November may be due to the tendency for a stronger response to El Nino and La Nina conditions in the winter (e.g., July) than in the summer (e.g., November). The SST areas with the strongest and most persistent correlations are to the east of Australia (negative correlations) and in the central south Pacific (positive correlations). We evaluated both of these regions for their potential as predictors using hindcasts based on the tercile matching method. For brevity, only the results from the positively correlated region (red boxes in Figure 33), which we will now refer to as the south Pacific SST predictor, are presented.

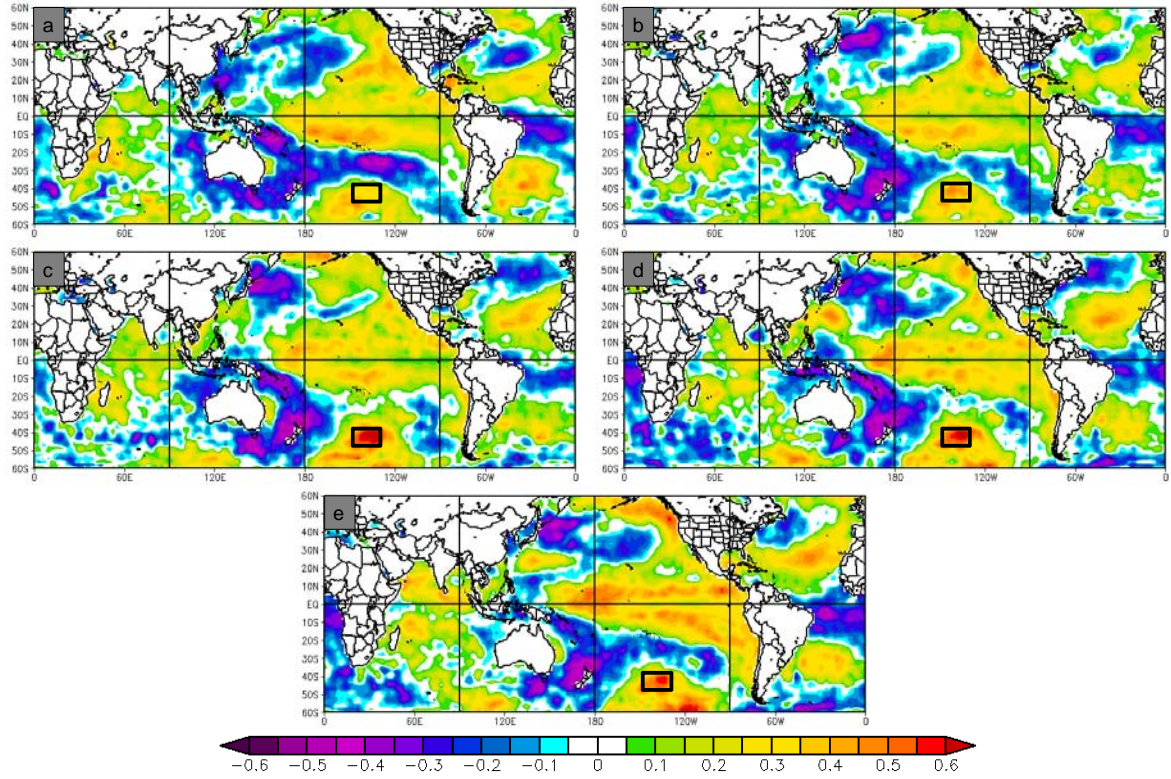


Figure 33. Correlations between November NAX SLD predictand and SST in: (a) November; (b) October; (c) September; (d) August; and (e) July based on data from 1970–2006. A positively correlated region (38° – 47° S, 210° – 230° E) in the Pacific was chosen as a potential predictor (black boxes).

Figure 34 shows time series of the NAX SLD predictand and the corresponding south Pacific SST predictor. Note that the predictand and predictor are generally in phase, as expected from the positive correlations shown in Figure 33. The two SST time series show a moderate amount of persistence from July to November, consistent with the persistence in the corresponding correlations (Figure 33), and favorable for long lead forecasting based on SST in this region. Notice also that there is significant sea surface temperature variation between July, when surface temperatures are cooler in the southern hemisphere winter, and November, when surface temperatures are warmer in the southern hemisphere summer. The time series show no strong

trend in the predictor or predictand, indicating that trends do not need to be accounted for when creating long-range composite analysis forecasts for the November 2009 ANNUALEX region.

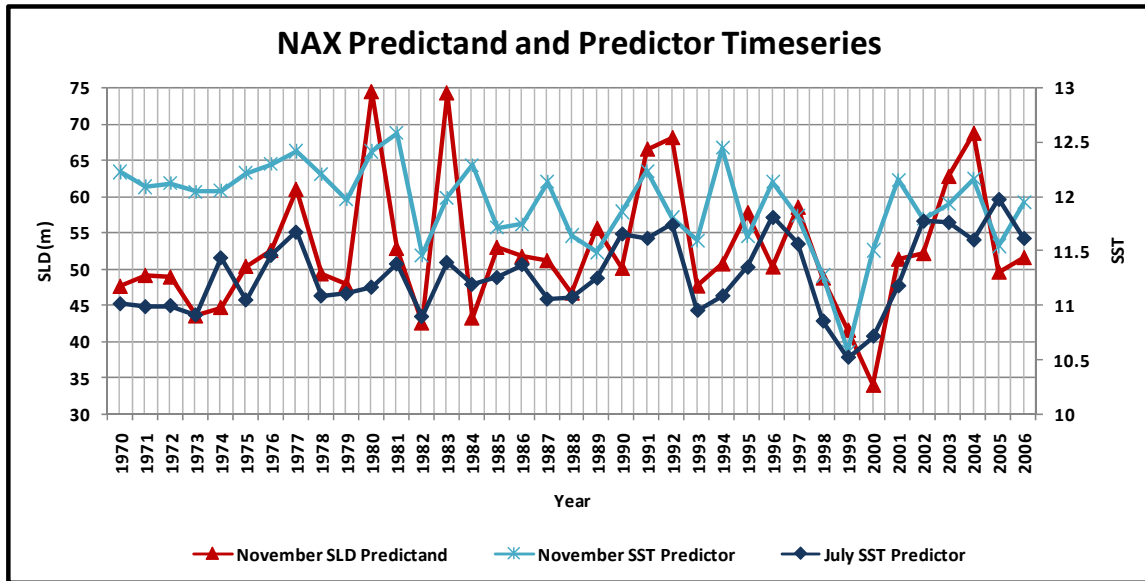


Figure 34. Time series of November ANNUALEX SLD predictand (NAX, red line), November south Pacific SST predictor (light blue line), and July south Pacific SST predictor (dark blue line) for 1970–2006.

Based on our correlation results, we applied the tercile matching method to determine the viability of our selected predictor-predictand pair (Table 4). Compared to our ECS predictand-predictor pair, the HSS values are not as high, but our percent correct for each lead time was greater than 0.50 and increasing out to longer lead times. This gave us confidence that this predictor-predictand pair was viable, and could be used in the CAF process to generate skillful long lead probabilistic forecasts for the November 2009 ANNUALEX.

Table 4. Contingency table results and verification metrics from hindcasts generated using the tercile matching method. Hindcasts of 1970–2006 NAX SLD predictand based on south Pacific SST predictor, with predictor leading by zero to four months. Columns A, B, C, and D represent the number of hits, false alarms, misses, and correct rejections respectively for AN, BN, and NN SLD values. See Chapter II, section D7, for details on contingency table and verification metrics.

	A	B	C	D	VERIFICATION METRICS			
	Hits	FA	Misses	Corr. Rej.	% Corr	FA Rate	POD	HSS
NOV South Pacific SST Predictor VS. NAX SLD Predictand Index								
AN SLD	5	7	7	18	0.622	0.583	0.417	0.218
BN SLD	6	6	6	19	0.676	0.500	0.500	0.320
NN SLD	5	8	8	16	0.568	0.615	0.385	0.154
OCT South Pacific SST Predictor VS. NAX SLD Predictand Index								
AN SLD	6	6	6	19	0.676	0.500	0.500	0.320
BN SLD	6	6	6	19	0.676	0.500	0.500	0.320
NN SLD	4	9	9	15	0.514	0.692	0.308	0.063
SEP South Pacific SST Predictor VS. NAX SLD Predictand Index								
AN SLD	9	3	3	22	0.838	0.250	0.750	0.645
BN SLD	8	3	4	22	0.811	0.273	0.667	0.579
NN SLD	8	6	5	18	0.703	0.429	0.615	0.406
AUG South Pacific SST Predictor VS. NAX SLD Predictand Index								
AN SLD	8	4	4	21	0.784	0.333	0.667	0.533
BN SLD	9	3	3	22	0.838	0.250	0.750	0.645
NN SLD	7	6	6	18	0.676	0.462	0.538	0.346
JUL South Pacific SST Predictor VS. NAX SLD Predictand Index								
AN SLD	6	6	6	19	0.676	0.500	0.500	0.320
BN SLD	9	3	3	22	0.838	0.250	0.750	0.645
NN SLD	4	9	9	15	0.514	0.692	0.308	0.063

Figure 35 shows a composite analysis (panel a) and two probabilistic long-range hindcasts (panels b and c) of sonic layer depth for our chosen sub-region of the ANNUALEX OPAREA in November based on our July south Pacific SST predictor. The statistically significant results (outlined in black or indicated by a black arrow) are for AN SST and BN SLD, BN SST and AN SLD, and BN SST and BN SLD. In Figure 35 (panel a), we also see a general pattern indicating highest (lowest) probability of BN SLD conditions when there are BN SST (AN SST) conditions in the predictor region and higher (lower) probability of AN SLD conditions when there are AN SST (BN SST) conditions in the predictor region. This of course is consistent with the correlations and tercile matching results

(Figures 33–34 and Table 4). The probabilistic long-range hindcasts in panels b and c indicate that the CAF process may be used to generate skillful long lead probabilistic forecasts of the November ANNUALEX sub-region using July SST conditions in the south Pacific predictor region. Panel b indicates that, based on BN July SST conditions, there is a 75 percent probability of BN, 25 percent probability of NN, and 0 percent probability of AN SLD conditions in the NAX predictand region in November. Panel c indicates that, based on AN July SST conditions there is a 50 percent probability of AN, 50 percent probability of NN, and 0 percent probability of BN SLD conditions in the NAX predictand region in November.

Note that a 50 percent probability of AN or NN SLDs indicates a much higher probability than normal of these sonic layer depths occurring. This is because in a tercile based analysis and forecasting approach, the normal probabilities are 33 percent for each tercile. To see that this situation is much different than normal, note that the probability of BN SLD is much lower than normal (zero percent). For operational use, it would be important for forecast users to understand and distinguish between tercile based probabilities for which the normal percentages are 33 percent for all categories, and more familiar bicile based probabilities (e.g., coin flip probabilities) for which the normal probabilities are 50 percent.

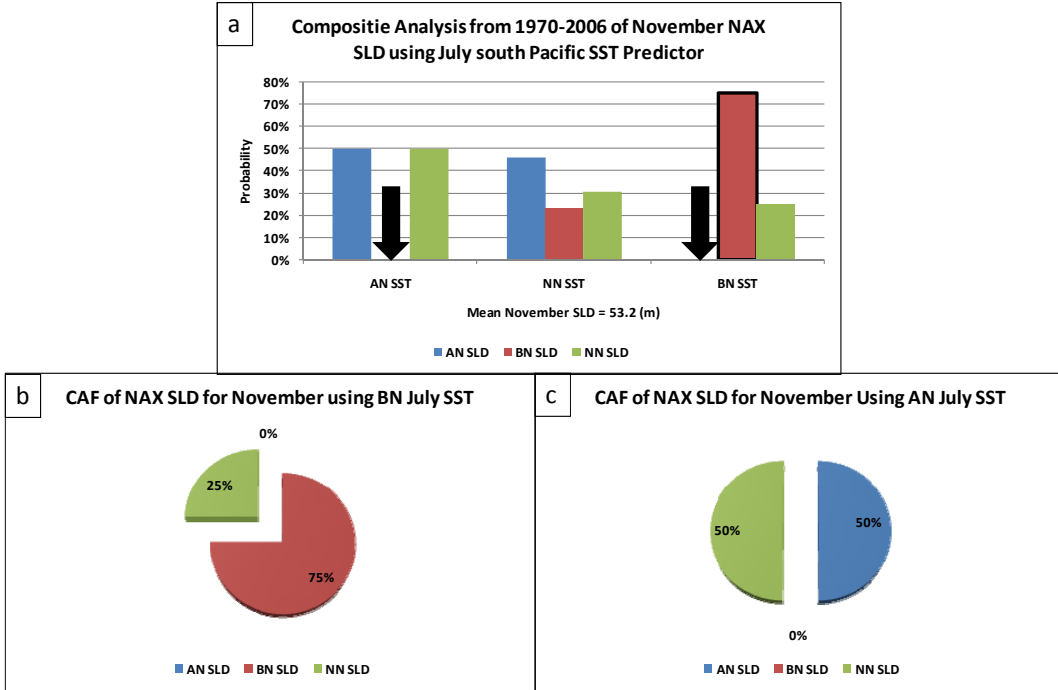


Figure 35. (a) Composite analysis for November SLD in ANNUALEX sub-region (NAX) using the south Pacific SST predictor in July. Statistically significant results are outlined in black or indicated by black arrows. (b) Corresponding probabilistic long-range hindcast of NAX SLD in November based on BN south Pacific SST predictor conditions in July. (c) Corresponding probabilistic long-range hindcasts of NAX SLD in November based on AN south Pacific SST predictor conditions in July. Thus, our CAF prediction of November 2009 NAX SLD based on AN July 2009 south Pacific SST conditions is: probability of above normal SLD—50%; probability of near normal SLD—50%; and probability of below normal SLD—0%.

Based on AN July SST anomalies (see Figure 26) in our south Pacific predictor region, our probabilistic long-range forecast of November 2009 NAX sonic layer depth issued in July 2009 would be similar to the CAF in panel c of Figure 35. Thus, ANNUALEX 2009 planners and decision makers can expect in November 2009, in the NAX sub-region (red box in Figure 32) a 50 percent probability of AN, 50 percent probability of NN, and 0 percent probability of BN sonic layer depths, based on a mean SLD value of 53 meters.

Knowing that our predictor-predictand pair is able to provide skillful probabilistic forecasts, we compared conditional composites of upper and lower tercile July SST predictor years with conditional mean composites of upper and lower November SLD predictand years (Figure 36). Figure 36 shows that the results based on using July SST predictor years to composite expected BN (lower tercile) and AN (upper tercile) November SLD conditions (i.e., the predicted composites) are similar to those based on using November SLD predictand years to composite actual BN (lower tercile) and AN (upper tercile) SLD conditions (i.e., to generate the actual or validating predictand composites). Panels a and b in Figure 36 are composites of lower tercile July SST predictor years and November SLD predictand years respectively. Notice that both panels are similar, which means that the years when SST was in the lower tercile for our July predictor are nearly the same as the years when SLD for our November predictand were in the lower tercile. The same is true for panel c and d in Figure 36, which are composites of upper tercile July SST predictor years and November SLD predictand years respectively. Figure 36 supports the use of our predictor-predictand pair for long lead SLD prediction.

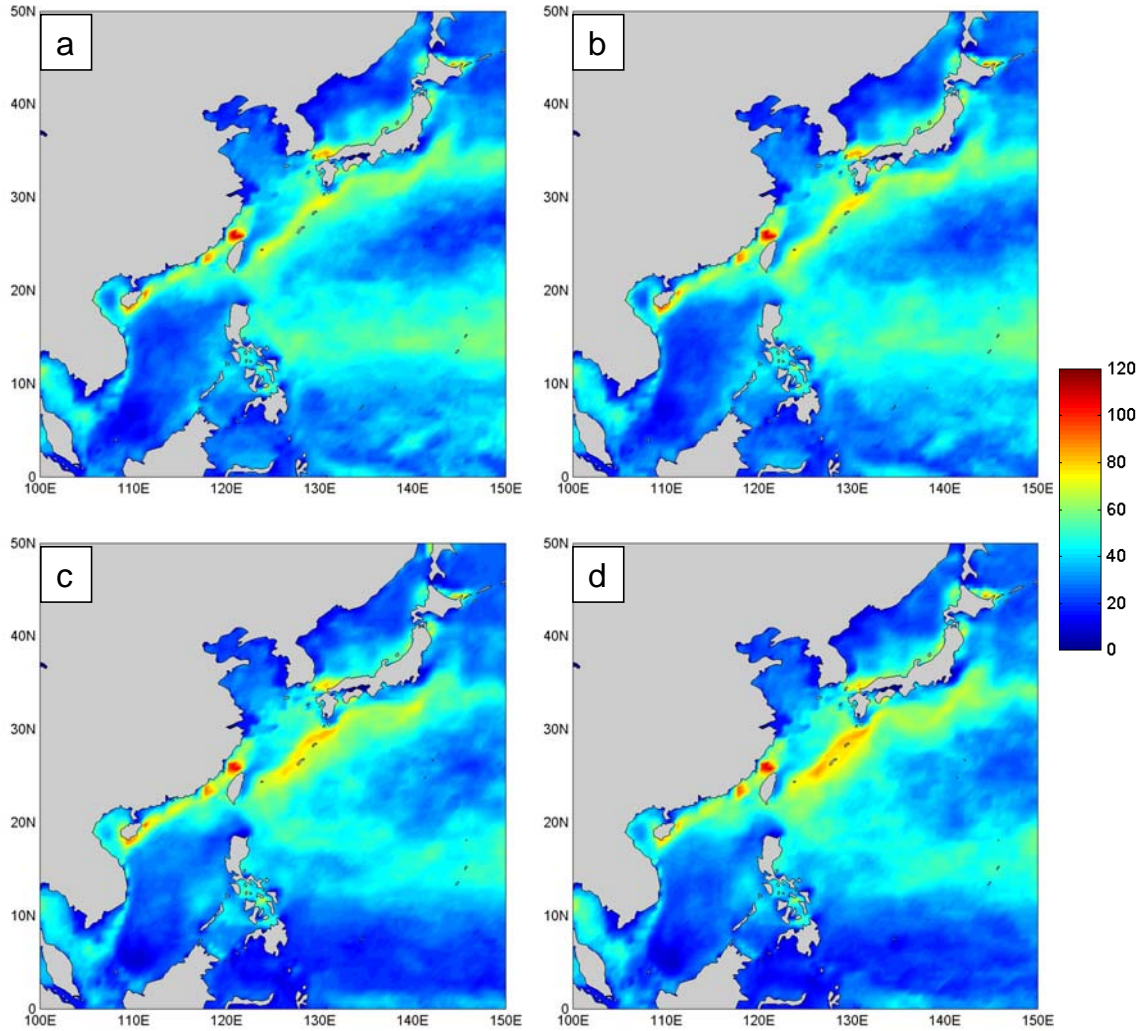


Figure 36. Conditional mean of November SLD based on compositing: (a) lower tercile July SST predictor years; (b) lower tercile November SLD predictand years; (C) upper tercile July SST predictor years; and (d) upper tercile November SLD predictand years.

Given our probabilistic long lead forecast for AN NAX SLD in November 2009 based on AN analyzed July 2009 SST in our predictor region, we composited upper tercile July SST predictor years to create conditional environmental threshold probability maps of SLD for November 2009. For comparison, we did the same for upper tercile November SLD predictand years. The results are shown in Figures 37 and 38. Note that for each threshold comparison between July SST predictor years and November SLD predictand years, there are only small differences in the overall probability patterns.

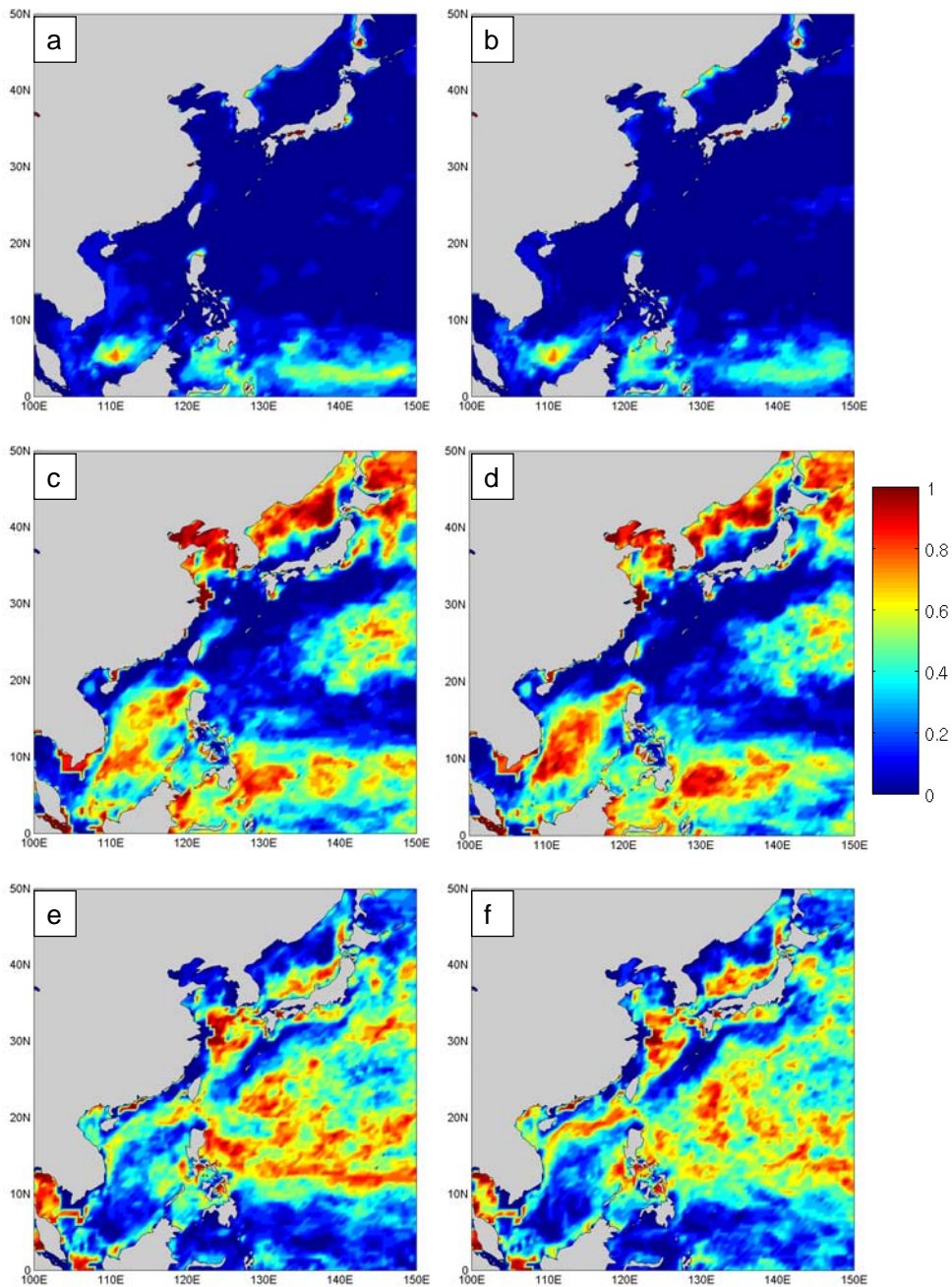


Figure 37. November SLD threshold probabilities based on upper tercile July SST predictor years and upper tercile November SLD predictand years. Probability of SLD: (a) less than or equal to 5 meters using July SST predictor; (b) less than or equal to 5 meters using November SLD predictand; (c) greater than 5 meters and less than or equal to 25 meters using July SST predictor; (d) greater than 5 meters and less than or equal to 25 meters using November SLD predictand; (e) greater than 25 meters and less than or equal to 46 meters using July SST predictor; (b) greater than 25 meters and less than or equal to 46 meters using November SLD predictand.

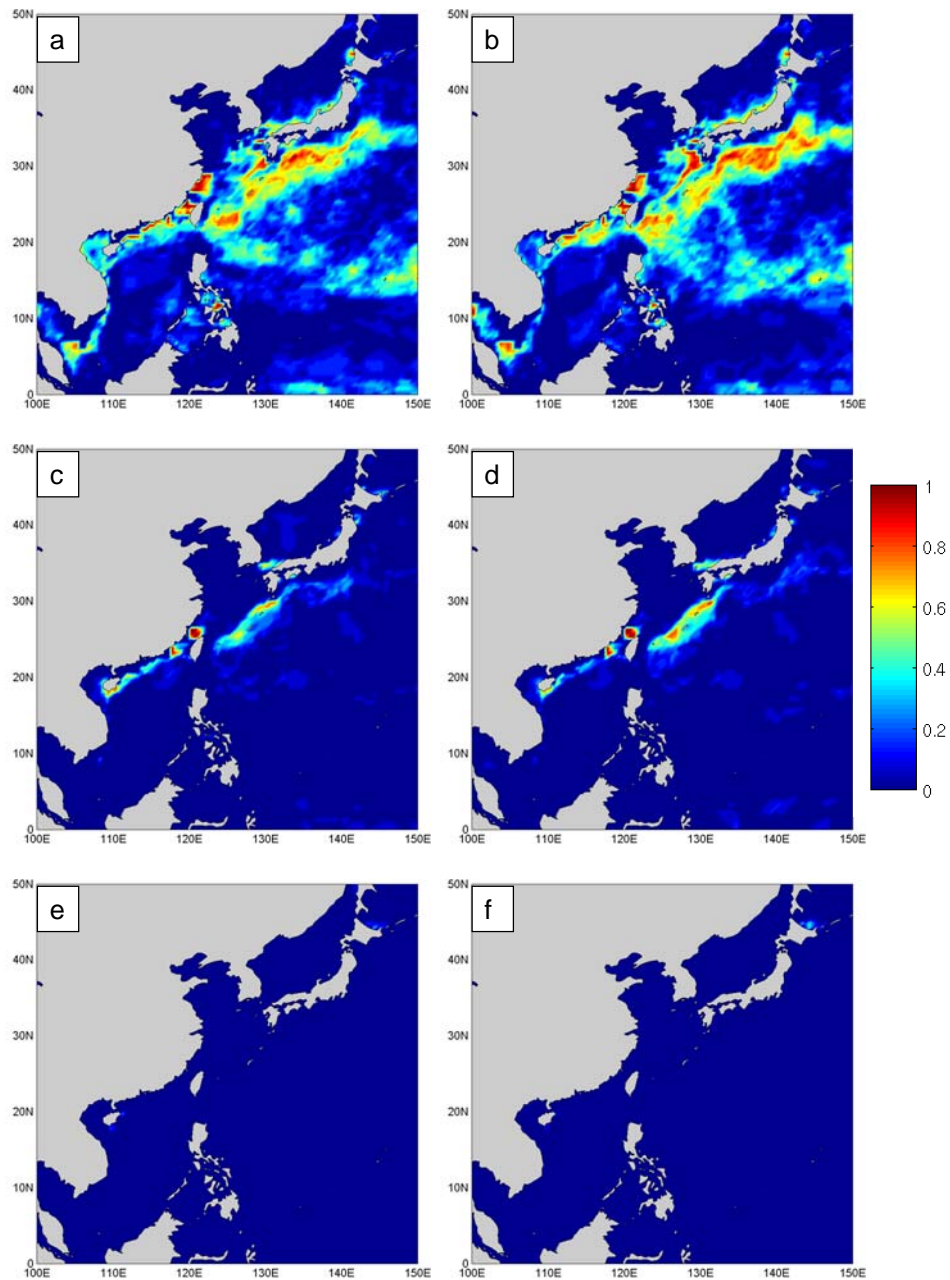


Figure 38. November SLD threshold probabilities based on upper tercile July SST predictor years and upper tercile November SLD predictand years. Probability of SLD: (a) greater than 46 meters and less than or equal to 70 meters using July SST predictor; (b) greater than 46 meters and less than or equal to 70 meters using November predictand; (c) greater than 70 meters and less than or equal to 112 meters using July SST predictor; (d) greater than 70 meters and less than or equal to 112 meters using November SLD predictand; (e) greater than 112 meters using July SST predictor; and (f) greater than 112 meters using November SLD predictand.

Figure 37 and Figure 38 support the validity of our predictor predictand pair. However, the small differences between the expected and validating threshold probabilities indicate that, while July south Pacific SST is a skillful predictor of November WNP SLD in this case, there are other variables factoring into the determination of sonic layer depth (e.g., SST in other regions).

C. LONG-RANGE FORECASTS OF SONAR PERFORMANCE

The results in the previous section are examples of climate scale tier one products in the Battlespace on Demand concept. These products were developed using advanced climate datasets (tier zero), and advanced analysis and forecasting methods (tier 1). Tier one products characterize the analyzed and predicted environment, and give decision makers the environmental awareness necessary for planning operations. The next step would be to use our long-range forecasts to develop tier two products that predict the performance of sonar and other equipment in the forecasted environment.

In Turek (2008), sonic layer depths for the East China Sea region from both GDEM and SODA climatology datasets were input into a Navy tactical decision aid to yield sonar performance predictions. Turek's results showed that climate variations in sound speed profiles and sonic layer depth can have large impacts on sonar performance. Based on Turek's work evaluating sensor performance of individual sonic layer depth profiles, we would expect similar impacts from the variations we have analyzed and forecasted. Future work evaluating sonar performance based on results from this study could lead to skillful climate scale tier two forecast products for long lead USW planning support.

IV. CONCLUSION

A. KEY RESULTS AND CONCLUSIONS

This study explored the viability of employing advanced climate datasets and methods to develop skillful long lead probabilistic forecasts of sonic layer depth in the western north Pacific. The primary focus of this work was to generate long lead climate support products for USW operations that offer a significant improvement in environmental awareness for Navy planners and decision makers.

Our proposed method (outlined in Chapter II) uses existing, and freely available state of the science atmospheric and oceanic reanalysis datasets to conduct analyses of long term means and climate variations in sonic layer depth. These analyses enabled us to identify intraseasonal to interannual climate patterns and processes within the western north Pacific associated with variations in sonic layer depth. Based on U.S. Navy operational interests, we selected two sub-regions within the western north Pacific for determination of long lead predictability potential. We correlated each WNP sub-region with potential predictor variables, and found sea surface temperature in the equatorial and south Pacific to have the strongest teleconnections with sonic layer depth at zero to four month lead times. Using a tercile matching method, we conducted hindcasts for 1970–2006 as a test of the viability of the SSTs as predictors of SLD in the sub-regions. If a selected predictor-predictand pair met specific criteria (see Chapter II, section D7), then a hypergeometric distribution method was used to test for statistical significance. Statistically significant relationships between the predictor and predictands were used to generate long lead probabilistic hindcasts. Based on analyzed sea surface temperature for July 2009, long lead probabilistic climate forecasts of sonic layer depth were generated in August 2009 for the East China Sea and ANNUALEX predictand regions in October and November 2009, respectively.

Conditional compositing techniques were exploited to develop additional long lead climate support products. Conditional composite means of upper and lower tercile predictand and predictor years help quantify the uncertainties in our long-range forecasts of sonic layer depth. Conditional environmental threshold probabilities based on long term mean and on upper and lower tercile categories provide additional support for long-range USW planning.

Our results indicate that skillful long-range probabilistic forecasts of sonic layer depth in the western north Pacific may be possible via prediction of individually identified sea surface temperature predictors within the Pacific (and possibly other predictors within other regions). While our results show a definite correlation between sea surface temperature in the equatorial and south Pacific and sonic layer depth in the western north Pacific, we suspect that there are additional factors and dynamics, which play an important role in the variability of sonic layer depth in the WNP. Our study is meant to highlight the predictive potential of our method and to show how using advanced datasets and methods to generate long-range forecasts of the ocean, and sonar performance, can enhance warfighter awareness and planning.

B. APPLICABILITY TO DOD OPERATIONS

The majority of day-to-day military scheduling and planning for USW exercises and operations begins several weeks to months prior to commencement. However, the Navy METOC community primarily focuses on short range forecasting support (lead times of 72 hours or less). Very few operational DoD products exist to aid USW mission planners in assessing and characterizing the likely state of the acoustic environment at lead times of weeks to months in advance, except for antiquated LTM based climatologies. Some experimental analysis products are being explored. But, to the best of our knowledge, no true long-range forecasts are available in operational or experimental form.

The USW planning phase, which occurs many months prior to the start of an operation, is arguably the phase when ocean climate support may have the greatest positive impact on USW operations, by alerting planners to the potential conditions that may impact their operations while there is still time to mitigate these impacts and exploit opportunities provided by other environmental conditions. Often times, short range forecasts come too late in the planning process to have much influence. In many of these cases, skillful long-range forecasts (e.g., lead times of two weeks or longer) could be very useful in exploiting the acoustic environment to give warfighters the USW advantage, such as determining when and where to conduct an operation, what sensors to deploy, and what tactics to employ. Additionally, better long-range planning has the potential for saving the military time and tax dollars.

Due to the lack of available long lead forecasting products, it is even more important for the Navy METOC community to provide state of the science climatology products that provide a comprehensible depiction of ocean climate and climate variations. Traditional LTM climatology datasets, such as GDEM, do not accurately depict climate variations, which, if not accounted for during planning and decision making phases, can have adverse affects on military operations. The studies by Moss (2007), Hanson (2007), Crook (2009), Tournay (2008), Mundhenk (2009), and others, along with results from this study, highlight the importance of using advanced climate datasets and methods to provide more complete and accurate forecasts than the current practice of using LTM based products for long-range military planning.

C. AREAS FOR FURTHER RESEARCH

Based on results from this study, it is evident that advanced climate datasets and methods can provide an immediate means of improved long lead climate support for USW planning and operations. This section highlights areas of future research to support these improvements.

1. The experimental long-range forecasts and other long lead planning products developed in this study should be provided to USW METOC support staff and USW planners for experimental use in USW planning. The results of that use should be assessed to determine how to improve product content, format, delivery, and timing.
2. This study focused primarily on using SLD as the predictand. To increase the operational relevance of this research, other predictands should be used, including BLG, ILG, and COF.
3. The datasets and methods used in this study of the WNP should be applied to other tactically significant and strategically important regions of the world.
4. This study focused primarily on using SST from individual regions as the predictor variable. SST from multiple regions, plus other oceanic variables (subsurface ocean temperature) should also be investigated as potential predictors.
5. This study focused on development of tier one products in the Battle Space on Demand concept. We recommend using the results from this study to develop tier two performance predictions and tier three decision recommendations for USW operations. Tier two products might consist of sonar performance forecasts based on PC-IMAT, to give USW planners estimated sonar ranges based on area of operations, characterization of the environment, sensor operating frequencies, and sensor deployment depths. Tier three products might consist of courses of action for USW planners based on environmental characterization, battle group assets, sensor deployment, and expected enemy actions.
6. This study primarily focused on statistical links between acoustically derived USW variables of interest and global climate variables. Future research should focus on developing a deeper understanding of the dynamics that cause

the teleconnections identified in this study, as done in, for example, Vorhees (2006), Hanson (2007), Moss (2007), Twigg (2007), and Crook (2009) .

7. Further research should be conducted to verify the composite analysis forecast method used to develop long lead probabilistic predictions of WNP sonic layer depth in this study. We recommend verification using extensive hindcasts and real forecasts.

8. A large amount of time for this study was spent manipulating data into a user friendly formats (especially the ocean reanalysis data). The methods used in this study could be applied much more efficiently and quickly if a web-based application was available for accessing, plotting, and analyzing the atmospheric and oceanic reanalysis data, and calculating derived quantities such as sound speed, SLD, BLG, etc. This would make climate datasets and methods much more available for research and operations (e.g., for identifying the primary long lead relationships for a specific area of interest). The ESRL applications for working with atmospheric reanalysis data are good examples of what is needed for all types of climate data.

THIS PAGE INTENTIONALLY LEFT BLANK

LIST OF REFERENCES

APDRC, cited 2009a: Asia-Pacific Data-Research Center: SODA v2.0.2. [Accessed online at http://apdrc.soest.hawaii.edu/datadoc/soda_pop2.0.2.htm.] Accessed August 2009.

APDRC, cited 2009b: Asia-Pacific Data-Research Center: SODA v2.0.4. [Accessed online at http://apdrc.soest.hawaii.edu/datadoc/soda_pop2.0.4.htm.] Accessed August 2009.

Carnes, M.R., 2003: Description and Evaluation of GDEM—V 3.0, OAML CIDREP review, 24 pp.

Carton, J.A., and B. Giese, 2008: A Reanalysis of ocean climate using Simple Ocean Data Assimilation. *Mon. Weather Rev.*, **136**, 2999–3017.

Carton, J.A., G. Chepurin, X. Cao, and B. Giese, 2000: A Simple Ocean Data Assimilation analysis of the global upper ocean 1950–95. Part I: Methodology. *Journal of Physical Oceanography*, **30**, 294–309.

CCSP, cited 2009: Climate glossary. [Accessed online at <http://www.cpc.ncep.noaa.gov/products/outreach/glossary.shtml>.] Accessed July 2009.

Crook, J., 2009: Climate analysis and long-range forecasting of dust storms in Iraq. M.S. Thesis, Dept. of Meteorology, Naval Postgraduate School, 85 pp.

Evans, Ashley, CDR, USN, 2007: *Battlespace On Demand – Command Brief*. Strike Group Oceanography Team San Diego, California, 21 pp.

Earth Systems Research Laboratory (ESRL), cited 2009. [Accessed online at <http://www.cdc.noaa.gov/cgi-bin/PublicData/getpage.pl>.] Accessed March 2009.

Federation of American Scientists (FAS), cited 2009: Introduction to Naval Weapons Engineering: Sonar Propagation. [Accessed online at http://www.fas.org/man/dod-101/navy/docs/es310/SNR-PROP/snr_prop.htm.] Accessed June 2009.

FOAL EAGLE 09 Critical Features Assessment, 2009. *Foal_Eagle09_Climo Mid-Planning_24NOV08.ppt*, 13 pp.

Ford, B., 2000: El Nino and La Nina Events, and tropical cyclones: impacts and mechanisms. M.S. Thesis, Dept. of Meteorology, Naval Postgraduate School, 120 pp.

Fox, D.N., and Coauthors, 2002: The Modular Ocean Data Assimilation System (MODAS). *Journal of Atmospheric and Oceanic Technology*, **19**(2), 240–252.

Google, cited 2009: Google Maps. [Accessed online at <http://maps.google.com/maps>.] Accessed May 2009.

Hanson, C., 2007: Long-range operational military forecasts for Iraq. M.S. Thesis, Dept. of Meteorology, Naval Postgraduate School, 77 pp.

John C Stennis USWEX/Deployment, 2009.
Optimized_JCS_PREBRIEF_USWEX.ppt, 12 pp.

Joint Staff, 2008: *Joint Publication 3–59: Meteorological and Oceanographic Operations*. U.S. Joint Chiefs of Staff, 24 September 2008, 87 pp.

Kalnay, E., and Coauthors, 1996: The NCEP/NCAR 40-year reanalysis project. *Bull. Amer. Meteor. Soc.*, **77**, 437–471.

Krynen, D., 2009: Personal communication.

LaJoie, M., 2006: The impact of climate variations on military operations in the Horn of Africa. M.S. Thesis, Dept. of Meteorology, Naval Postgraduate School, 153 pp.

Mackenzie, K.V., 1981: Nine-term equation for the sound speed in the oceans. *J. Acoust. Soc. Am.* **70**(3), 807–812.

MetEd, cited 2009: Creating a Local Climate Product Using Composite Analysis. [Accessed online at <http://www.meted.ucar.edu/climate/composite/print.htm>.] Accessed May 2009.

Moss, S.M., 2007: Long-range operational military forecasts for Afghanistan. M.S. Thesis, Dept. of Meteorology, Naval Postgraduate School, 99 pp.

Mundhenk, B., 2009: A statistical-dynamical approach to intraseasonal prediction of tropical cyclogenesis in the western north Pacific. M.S. Thesis, Dept. of Meteorology, Naval Postgraduate School, 129 pp.

Murphree, T., 2008: *MR3610 Course Module 6: Smart Climatology*. Dept. of Meteorology, Naval Postgraduate School, Monterey, California, 52 pp.

Naval Oceanography Portal (UNCLASS), cited 2009. [Accessed online at: <http://nop.oceanography.navy.smil.mil/Content/organization/production-centers/navo/PRODUCTS/MODEL/NOSSP-Global-NCOM-Products.>] Accessed July 2009.

Open University, 2001. *Ocean Circulation*, 2nd Edition, Butterworth-Heinemann Press, 242 pp.

Ramsaur, D.C., 2009: Climate analysis and long-range forecasting of radar performance in the Western North Pacific. M.S. Thesis, Dept. of Meteorology, Naval Postgraduate School, 115 pp.

Raynak, C., 2009: Statistical-dynamical forecasting of tropical cyclogenesis in the north Atlantic at intraseasonal lead times. M.S. Thesis, Dept. of Meteorology, Naval Postgraduate School, 93 pp.

Rhodes, R.C., and Coauthors, 2002: Navy real-time global modeling systems. Special Issue – Navy Operational Models: Ten Years Later, *Oceanography*, **15**(1), 29–43.

Tomczak, M., and Godfrey, J.S., 2003: *Regional Oceanography: an Introduction* 2nd edn, 390 pp.

Tournay, R., 2008: Long-range forecasting of Korean summer precipitation. M.S. Thesis, Dept. of Meteorology, Naval Postgraduate School, Monterey, California, 121 pp.

Turek, A., 2008: Smart climatology applications for Undersea Warfare. M.S. Thesis, Dept. of Meteorology, Naval Postgraduate School, Monterey, California, 95 pp.

Twigg, K.L., 2007: A smart climatology of evaporation duct height and surface radar propagation in the Indian Ocean. M.S. Thesis, Dept. of Meteorology, Naval Postgraduate School, Monterey, California, 135 pp.

Vorhees, D., 2006: The impacts of global scale climate variations on Southwest Asia. M.S. Thesis, Dept. of Meteorology, Naval Postgraduate School, 175 pp.

Wilks, D., 2006: *Statistical Methods in the Atmospheric Science*, Academic Press, 627 pp.

THIS PAGE INTENTIONALLY LEFT BLANK

INITIAL DISTRIBUTION LIST

1. Defense Technical Information Center
Ft. Belvoir, Virginia
2. Dudley Knox Library
Naval Postgraduate School
Monterey, California
3. Dr. Tom Murphree
Naval Postgraduate School
Monterey, California
4. CAPT Robert Kiser
Naval Oceanography Operations Command
Stennis Space Center, Mississippi
5. CAPT Brian Brown
Naval Oceanographic Office
Stennis Space Center, Mississippi
6. CAPT (sel) Paul Oosterling
Naval Oceanography Operations Command
Stennis Space Center, Mississippi
7. CDR Rebecca Stone
Naval Postgraduate School
Monterey, California
8. CDR Tony Miller
Naval Oceanography ASW Center
Stennis Space Center, Mississippi
9. CDR Eric Trehubenko
Naval Oceanography ASW Center
Yokosuka, Japan
10. LCDR Tim Campo
Naval Oceanography Operations Command
Stennis Space Center, Mississippi
11. Dennis Krynen
Naval Oceanographic Office – Ocean Predictions Department
Stennis Space Center, Mississippi